



UNIVERSITÀ POLITECNICA DELLE MARCHE  
Repository ISTITUZIONALE

Assessment of intrinsic aquifer vulnerability at continental scale through a critical application of the drastic framework: The case of South America

This is the peer reviewed version of the following article:

*Original*

Assessment of intrinsic aquifer vulnerability at continental scale through a critical application of the drastic framework: The case of South America / Rama, F.; Busico, G.; Arumi, J. L.; Kazakis, N.; Colombani, N.; Marfella, L.; Hirata, R.; Kruse, E. E.; Sweeney, P.; Mastrocicco, M.. - In: SCIENCE OF THE TOTAL ENVIRONMENT. - ISSN 0048-9697. - ELETTRONICO. - 823:(2022). [10.1016/j.scitotenv.2022.153748]

*Availability:*

This version is available at: 11566/298652 since: 2024-07-17T10:10:04Z

*Publisher:*

*Published*

DOI:10.1016/j.scitotenv.2022.153748

*Terms of use:*

The terms and conditions for the reuse of this version of the manuscript are specified in the publishing policy. The use of copyrighted works requires the consent of the rights' holder (author or publisher). Works made available under a Creative Commons license or a Publisher's custom-made license can be used according to the terms and conditions contained therein. See editor's website for further information and terms and conditions.

This item was downloaded from IRIS Università Politecnica delle Marche (<https://iris.univpm.it>). When citing, please refer to the published version.

(Article begins on next page)

# ASSESSMENT OF INTRINSIC AQUIFER VULNERABILITY AT CONTINENTAL SCALE THROUGH A CRITICAL APPLICATION OF THE DRASTIC FRAMEWORK: THE CASE OF SOUTH AMERICA

Fabrizio Rama<sup>1\*</sup>, Gianluigi Busico<sup>2</sup>, José Luis Arumi<sup>3</sup>, Narantzis Kazakis<sup>4</sup>, Nicolò Colombani<sup>5</sup>, Luigi Marfella<sup>6</sup>, Ricardo Hirata<sup>7</sup>, Eduardo E. Kruse<sup>8</sup>, Paul Sweeney<sup>1</sup>, Micòl Mastrocicco<sup>2</sup>.

\* Corresponding author

<sup>1</sup>. Syngenta – Jealott’s Hill International Research Centre, Environmental Safety, Warfield, Bracknell RG426EY, United Kingdom

<sup>2</sup>. Department of Environmental, Biological and Pharmaceutical Sciences and Technologies, University of Campania “Luigi Vanvitelli”, Via Vivaldi 43, 81100 Caserta, Italy

<sup>3</sup>. Department of water resources, Faculty of Agriculture Engineering, Centro Fondap CRHIAM, University of Concepción, Chile

<sup>4</sup>. Department of Geology, Laboratory of Engineering Geology and Hydrogeology, Aristotle University of Thessaloniki, Thessaloniki, 54124, Greece.

<sup>5</sup>. Department of Materials, Environmental Sciences and Urban Planning, Polytechnic University of Marche, Via Brecce Bianche 12, 60131 Ancona, Italy.

<sup>6</sup>. School of Geography, Geology and the Environment, Keele University, Keele, Staffordshire ST5 5BG, United Kingdom

<sup>7</sup>. Institute of Geosciences, University of São Paulo (USP); Director CEPAS|USP: Groundwater Research Center; Vice-President of Brazilian Groundwater Association – ABAS; FAPESP Geosciences Coordinator, Sao Paulo (SP), Brazil

<sup>8</sup>. Consejo Nacional de Investigaciones Científicas y Técnicas (CONICET), Facultad de Ciencias Naturales y Museo, Universidad Nacional de La Plata (UNLP), Calle 64 #3 (entre 119 y 120), 1900, La Plata, Buenos Aires, Argentina

## HIGHLIGHTS:

- First map of intrinsic aquifer vulnerability of South America continent is provided
- Outcomes are validated by sensitivity analyses and previous regional assessments
- Extensive discussion about data collection and limits of DRASTIC method is provided
- The DRASTIC assessment shows a medium to low vulnerability at continental scale
- Results show a higher vulnerability of aquifers in Amazon compared to other regions

## ABSTRACT:

An assessment of the intrinsic aquifer vulnerability of South America is presented. The outcomes represent the potential sensitivity of natural aquifers to leaching of dissolved compounds from the land surface. The study, developed at continental scale but retaining regionally a high resolution, is based on a critical application of the DRASTIC method. The biggest challenge in performing such a study in South America was the scattered and irregular nature of environmental datasets. Accordingly,

37 the most updated information on soil, land use, geology, hydrogeology, and climate at continental,  
38 national, and regional scale were selected from international and local databases. To avoid spatial  
39 discrepancy and inconsistency, data were integrated, harmonized, and accurately cross-checked,  
40 using local professional knowledge where information was missing. The method was applied in a  
41 GIS environment to allow spatial analysis of raw data along with the overlaying and rating of maps.  
42 The application of the DRASTIC method allows to classify South America into five vulnerability  
43 classes, from very low to very high, and shows an overall medium to low vulnerability at continental  
44 scale. The Amazon region, coastal aquifers, colluvial Andean valleys, and alluvial aquifers of main  
45 rivers were the areas classified as highly vulnerable. Moreover, countries with the largest areas with  
46 high aquifer vulnerability were those characterized by extended regions of rainforest. In addition, a  
47 single parameter sensitivity analysis showed depth to water table to be the most significant factor,  
48 while a cross-validation using existing vulnerability assessments and observed concentrations of  
49 compounds in groundwater confirmed the reliability of the proposed assessment, even at regional  
50 scale. Overall, although additional field surveys and detailed works at local level are needed to  
51 develop effective water management plans, the present DRASTIC map represents an essential  
52 common ground towards a more sustainable land-use and water management in the whole territory  
53 of South America.

54

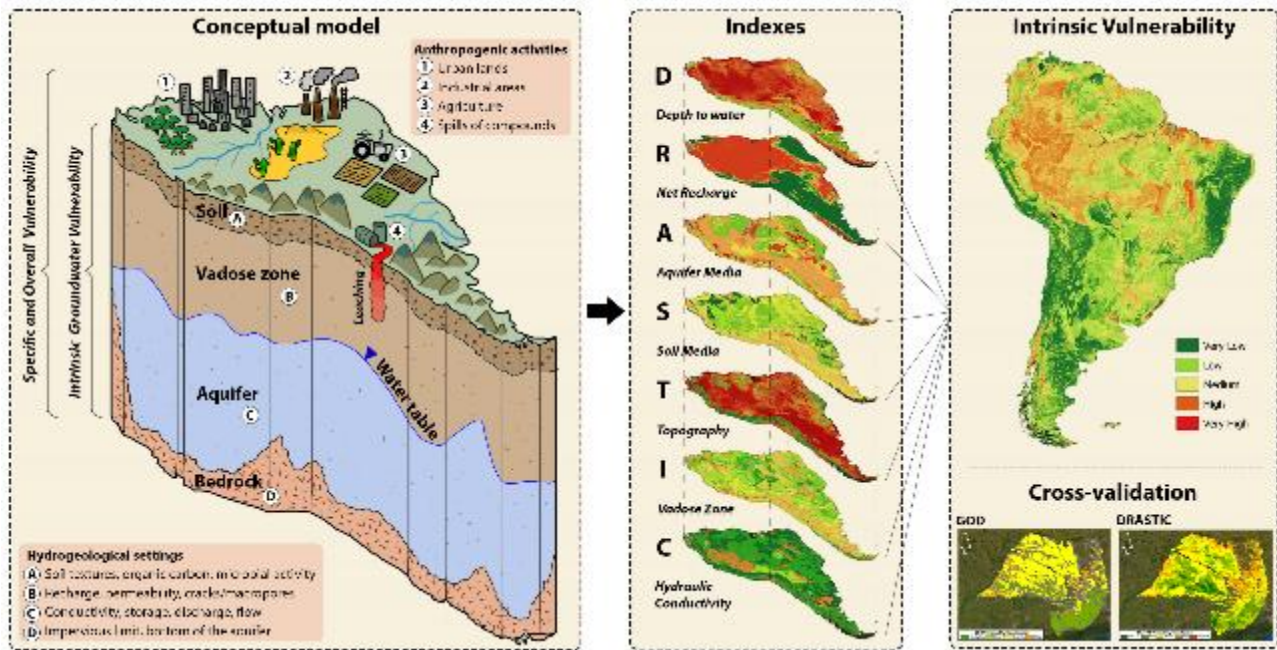
55 **Keywords:**

56 Intrinsic groundwater vulnerability; High-resolution maps; GIS; Groundwater; South America;  
57 DRASTIC

58

59 **GRAPHICAL ABSTRACT:**

60



## 1. INTRODUCTION

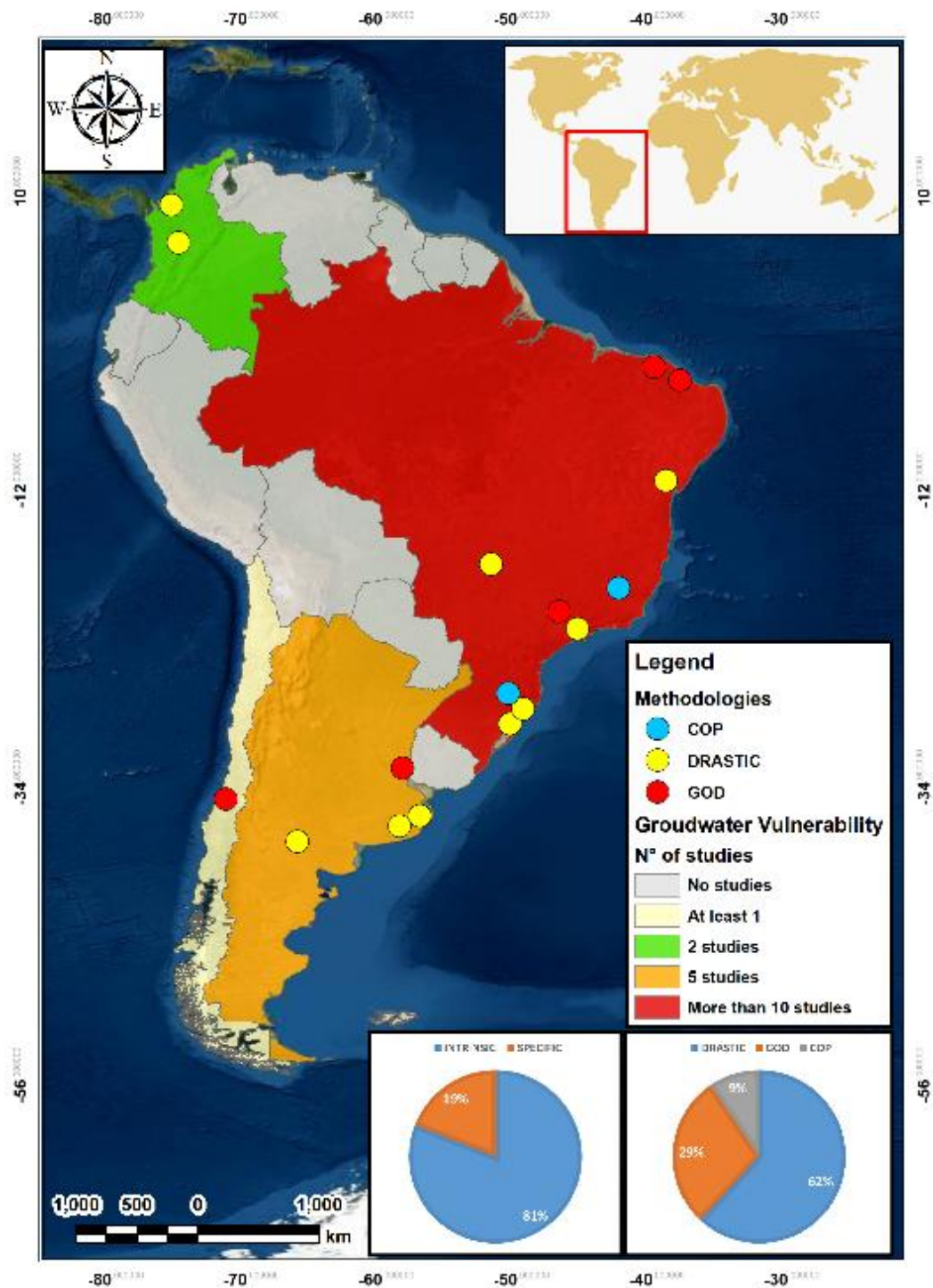
Groundwater is the largest store of available freshwater in the world (Cuthbert et al., 2019). Broadly, more than half of world's population depends on subsurface water for any kind of utilizations such as drinking, irrigation, domestic and industrial purposes (Oki and Kanae, 2006; Gleeson et al., 2010). It was accounted that this resource provides drinking water for two billion people and irrigation for 40% of cropland (Siebert et al., 2010; Jasechko et al., 2014). However, growing population and anthropogenic uses trigger depletion and pollution of this water resource, with clear detrimental effects at both regional and local scales (Aeschbach-Hertig and Gleeson, 2012). For example, aquifers in United States (US) have lost more than 700 km<sup>3</sup> of water during the twentieth century (Konikow and Kendy, 2005), and future long-term impacts of climate change may intensify this negative pattern. On top of that, aquifers in every part of the world receive today higher loads of anthropogenic substances, which may infiltrate through the unsaturated zone and accumulate deep in the subsurface system (Ascott et al., 2017; Jasechko et al., 2017). Groundwater is consequently a vital and fragile resource that requires a forward-looking approach in its management. In this framework, assessing aquifer vulnerability to leaching represents a key preventive tool in terms of screening and management to achieve a sustainable use of groundwater resources (Alley et al., 1999; Foster et al., 2013). Knowing the vulnerability of an aquifer in a specific location can help design tailored management plans and protection strategies, which balance wisely present development and future needs. The term aquifer vulnerability indicates the degree to which a subsurface system is likely to be adversely affected by any perturbation or stress from the land surface (Aller et al., 1987). It depends on the natural attenuation capacity related to a set of physicochemical processes in a certain location

(e.g. filtration, biodegradation, hydrolysis, adsorption, dilution, volatilization, and dispersion). Accordingly, intrinsic vulnerability refers to the natural protection afforded by local hydrogeological setting, while specific vulnerability also includes specific land uses, management practices, and chemical characteristics of the compounds (Stigter et al., 2006; Gimsing et al., 2019). Alternatively, for the latter case, some authors (Foster and Hirata, 1988; Foster et al., 2013) prefer the term aquifer hazard as an interaction between pollutant load activities and intrinsic aquifer vulnerability, recognizing that elevated hazard occurs only when a high pollutant load affects a highly vulnerable area. Aquifer vulnerability can be estimated using different approaches (US-NRC, 1993), which vary in terms of complexity, computation effort, and data requirement: (a) overlay/index methods, (b) process-based models, (c) statistical methods and, raised in the last two decades, (d) hybrid methods. “Index methods” classify main drivers of leaching process one-by-one (i.e. indexes), assigning a “rating” and sum them up with a linear combination in a GIS-environment (Gogu and Dassargues, 2000; Neshat et al., 2014; Massone and Barilari, 2020). They are simple and easy-to-use, generally require minimal data and are scalable to large domains but produce only single static value for vulnerability. For this reason, they are deployed as a screening tool for extended domains (e.g., regional to national). Conversely, “process-based methods” aim to develop a comprehensive and transient-over-time model of the natural domain, which is controlled by physically based relations (Wachniew et al., 2016). They are complex and powerful tools, but time and data consuming. Accordingly, they are mostly used on small domains (e.g., field to regional) as require extensive parametrization and high computational effort to obtain a strictly site-specific assessment. “Statistical methods” such as conditional probability analysis, weight of evidence (WOE) multiple linear regression (MLR) or geostatistical interpolation (kriging) define the vulnerability of an aquifer based on available observations rather than analysing natural mechanisms and local conditions (Roy-Roura et al., 2013; Busico et al., 2018; Javadi et al., 2020; Rahmani et al., 2021). They allow assessment of groundwater exposure and its uncertainty by processing large sets of data, but consequently, rely on availability and quality of that data, which can be difficult to obtain. Lastly, “hybrid methods” recombine previous approaches using recent numerical algorithms e.g. genetic algorithms, machine learning (Nadiri et al., 2018; Jahromi et al., 2021, Sadeghfam et al., 2021) or combining different modelling approaches (Keuskamp et al., 2012; Jia et al., 2019). They try to overcome the limitations of other methods by reducing the subjectivity of ratings and by modifying the limits of vulnerability classes. For example, DRASTIC and SINTACS were fully hybridized by a calibration process using parameter weights and scores (Kazakis and Voudouris, 2015; Busico et al., 2017; Busico et al., 2020). An exhaustive review of those approaches along with limitations and future challenges is available in Machiwal et al. (2018a; b) and Goyal et al. (2021). Most of the applicability of a specific method

depends on the availability and quality of data (i.e., observations of groundwater quality and local conditions to characterize the domain or constrain the model). Accordingly, simpler, and faster approaches, which require less data and time to run, are still the most employed worldwide. Index and rating methods such as DRASTIC (Aller et al., 1987), AVI (Van Stemproot et al., 1993), SINTACS (Civita and De Maio, 2004) and GOD (Foster, 1987; Foster and Hirata, 1988), COP (Vias et al., 2006) which summarize complex hydrogeological settings in few intuitive indexes, are the most applied for assessment of aquifer vulnerability of extended areas. In the last years, vulnerability assessments have started to be developed at very large scale in different parts of the world. Although lacking in a comprehensive continental map, North America and Asia boasted a considerable scientific production about aquifer vulnerability on international indexed journals, developing studies at very large scale (Fritch et al., 2000; Huan et al., 2012; Li and Merchant, 2013; Yin et al., 2013). At the same time, pan continental maps of groundwater vulnerability have been developed in Europe (Kumar et al., 2020; Nistor, 2020) and Africa (Ouedraogo et al., 2016). These assessments represented the initial attempts of using remote sensing and open data to estimate the aquifer vulnerability locally, but in a consistent continental framework. However, they missed an extensive discussion about limitations of the available datasets and the strong link of the results with the quality of input data. In addition, continental maps of groundwater vulnerability in Europe and Africa have pixel dimensions of about 15 km or more, which result in map scales lower than 1:60M. Nevertheless, territorial planning issues usually require cartographies with larger scales to allow municipal (e.g., 1:25k-1:50k) or state/provincial (e.g., 1:100k-1:500k) operators to correctly manage land use or establish priority-action policies for a sustainable groundwater management. This shift in map scaling may entail that academically valid contributions have in practice little scope in terms of management by authorities and policymakers. Given that a continental vulnerability assessment of groundwater is less well established in South America, the present paper aims to fill this gap. However, it aspires to do so, by providing a continental map that maximizes the local resolution of hydrogeological features. In South America, aquifer vulnerability started gaining visibility in scientific literature only in the last two decades, having most of the indexed works published in the last 10 years. Although land use change is a hot topic for groundwater depletion in South America (De Sy et al., 2015), aquifer vulnerability and water quality degradation represent two environmental topics only recently well understood (Bocanegra et al., 2010). Furthermore, availability of reliable and continuous datasets with environmental data is scarce and scattered. Accordingly, the spatial distribution of indexed vulnerability studies in South America is far from uniform (Fig. 1). Literature research on Scopus database (i.e. Elsevier) has showed that only Brazil, Argentina, Colombia, and Chile have at least one indexed study in English on groundwater vulnerability at local and regional scale (Table S0). Most

152 of the studies focused on Brazil and Argentina, which count more than ten and five studies,  
153 respectively. In Brazil, the two most applied methods are DRASTIC (Herlinger and Viero, 2007;  
154 Nobre et al., 2007; Seabra et al., 2009; Caprario et al., 2019; Giacomazzo and de Almeida, 2020) and  
155 GOD, (Hirata et al., 1991; Gomes et al., 2018; Peixoto and Cavalcante, 2019), followed by COP  
156 (Tayer and Velasquez, 2017; Aragão et al., 2020), which is specific for karst regions. The first and  
157 largest application of a rating method in South America was also in Brazil, where a GOD vulnerability  
158 assessment in 1991 was developed for the entire Sao Paulo state (Hirata et al., 1991). In Argentina,  
159 DRASTIC method is the most deployed for both, intrinsic (Massone et al., 2010; Montoya et al.,  
160 2019) or specific vulnerability (Lima et al., 2011), followed by GOD (Boujon and Sanci, 2014).  
161 Finally, Colombia (Betancur et al., 2013; Agudelo Moreno et al., 2020) and Chile (Duhalde et al.,  
162 2018) only showed two and one studies, respectively. Conversely, there are plenty of unindexed  
163 articles and reports in Portuguese and Spanish (roughly more than 1,000) using different assessment  
164 methods to address groundwater vulnerability at local scale. In many regions of Brazil, Costa Rica,  
165 Argentina, and Colombia, GOD is also used by governs and authorities as an official tool to control  
166 land use. Such a disjointed range of regional assessments would benefit from a pan continental study,  
167 which aims to harmonize vulnerabilities from different countries of South America in a common  
168 framework and to provide an international showcase for a large unpublished literature (i.e.  
169 government documents) on aquifer vulnerability. Moreover, in South America there are 29  
170 transboundary aquifers (IGRAC, 2015) and a pan continental study would also ease international  
171 cooperation on water resources management, promoting the sound development of joint projects  
172 specific to groundwater (Villar, 2016). Furthermore, none of the previous studies offered a robust  
173 validation of the proposed methodology or a quality check of the results. Accordingly, this paper  
174 presents the very first DRASTIC-based assessment of intrinsic groundwater vulnerability at  
175 continental scale in South America, which retains a high resolution of final maps. Local and  
176 international databases were combined to maximize spatial discretization and resolution of the  
177 proposed map in GIS (250m pixel resolution, which results in about 1:500k of map scale). In the  
178 manuscript, the authors go through a quality check of the input datasets used in the method, validate  
179 the vulnerability map against groundwater concentrations of different compounds (e.g.,  $\text{NO}_3^-$ ,  $\text{Cl}^-$ ,  
180  $\text{PO}_4^{3-}$ ) and previous assessments at local scale, and discuss main limitations of DRASTIC  
181 methodology. Only freely available sources and datasets were used in this work. The data collection  
182 is fully documented and stored in a dedicated repository (Rama et al., 2021).

183



184

185

186

187

188

189

## 2. STUDY AREA

190

191

192

**Fig. 1:** Distribution of local and regional studies on groundwater vulnerability in South America from a literature review. The review was conducted on Scopus database (Elsevier), focused on regional and local studies (Base map from ESRI Digital Globe 2021).

The study area is represented by the fourth largest continent in the world: South America (Fig. 2a). The continental limit is defined by the frontier between Colombia (in) and Panama (out), having as a Northernmost point Punta Gallinas, Colombia (12°27'31"N-71°40'8"W), Southernmost point Cape

193 Froward, Chile (53°53'47"S -71°17'40"W), Westernmost point Punta Pariñas, Peru (4°40'58"S-  
194 81°19'43"W) and Easternmost point Ponta do Seixas, Brazil (7°9'19"S-34°47'35"W). It includes 13  
195 countries (Argentina, Bolivia, Brazil, Chile, Colombia, Ecuador, Guyana, Paraguay, Peru, Suriname,  
196 Trinidad and Tobago, Uruguay, and Venezuela) and many other territories. Most of the continent is  
197 located above a large tectonic plaque, whose movement to West was producing the subduction of  
198 Nazca Plaque, which generated Andean Cordillera (Capitanio et al., 2011). Thus, from the  
199 hydrogeological point of view, the Andes divide South America into two major regions. On the one  
200 hand, the Pacific region (i.e., tectonically active), where basins and aquifers are relatively small, being  
201 limited by the topography of the intermontane valleys. On the other hand, the Atlantic region, which  
202 is tectonically inactive, hosts large basins (e.g., the Orinoco and Amazon systems), plains of  
203 extremely low slope (e.g., Chaco-Pampean plain in the Rio de la Plata basin), and transboundary  
204 groundwater bodies (e.g., Guaraní aquifer across Brazil, Uruguay, Paraguay, and Argentina).  
205 Accordingly, the map of groundwater resources (Fig. 2b) obtained from the World-wide  
206 Hydrogeological Mapping and Assessment Programme (WHYMAP) (Richts et al, 2011) shows that  
207 large groundwater basins, which include the entire Amazon basin in Brazil, Venezuela, and Guyana,  
208 along with the transboundary Guaraní aquifer system, are mainly located in the Atlantic region.  
209 Conversely, complex hydrogeological systems, which refer to fractured and karstified systems, and  
210 local aquifers are quite extensive in the Pacific side and on the top of Andean Cordillera. In addition,  
211 South America presents a slightly variable regime of temperature and precipitation on the land  
212 surface, having most of the climates of the world (Fig. 2b). The Andean Cordillera affects air mass  
213 circulation in atmosphere, intercepting most of the large rain systems from both sides associated with  
214 Atlantic Westerlies and Pacific Frontals systems (Garreaud et al., 2009). This interception produces  
215 intense rainfall concentrated in specific regions, for example the Orinoco-Amazonas watershed  
216 (Yoon et al., 2010), and the Paramos of the tropical Andes, which consequently represent important  
217 and fragile sources of freshwater (Céleri and Feyen, 2009). Conversely, those focused precipitations  
218 produce extremely dry areas, such as the Latin-American diagonal of aridity, which interest most of  
219 the cost of Peru, North and central Chile, and South Argentina (Núñez and Verbist, 2018). The wide  
220 variability of climate conditions in the continent is also affected by irregular and periodic large-scale  
221 variations in wind circulations, such as El Niño-Southern Oscillations (ENSO), the Pacific Decadal  
222 Oscillation and the Atlantic Oscillation (Garreaud, 2009). In terms of land use, about 50% of South  
223 America is covered by forests, followed by grasslands 26%, agriculture 24%, barren 3%, and water  
224 bodies 1% (Fig. 2c). Percentage of forests in each country ranges from 9.5% in Uruguay to 96.5% in  
225 French Guiana (Giri and Long, 2014).

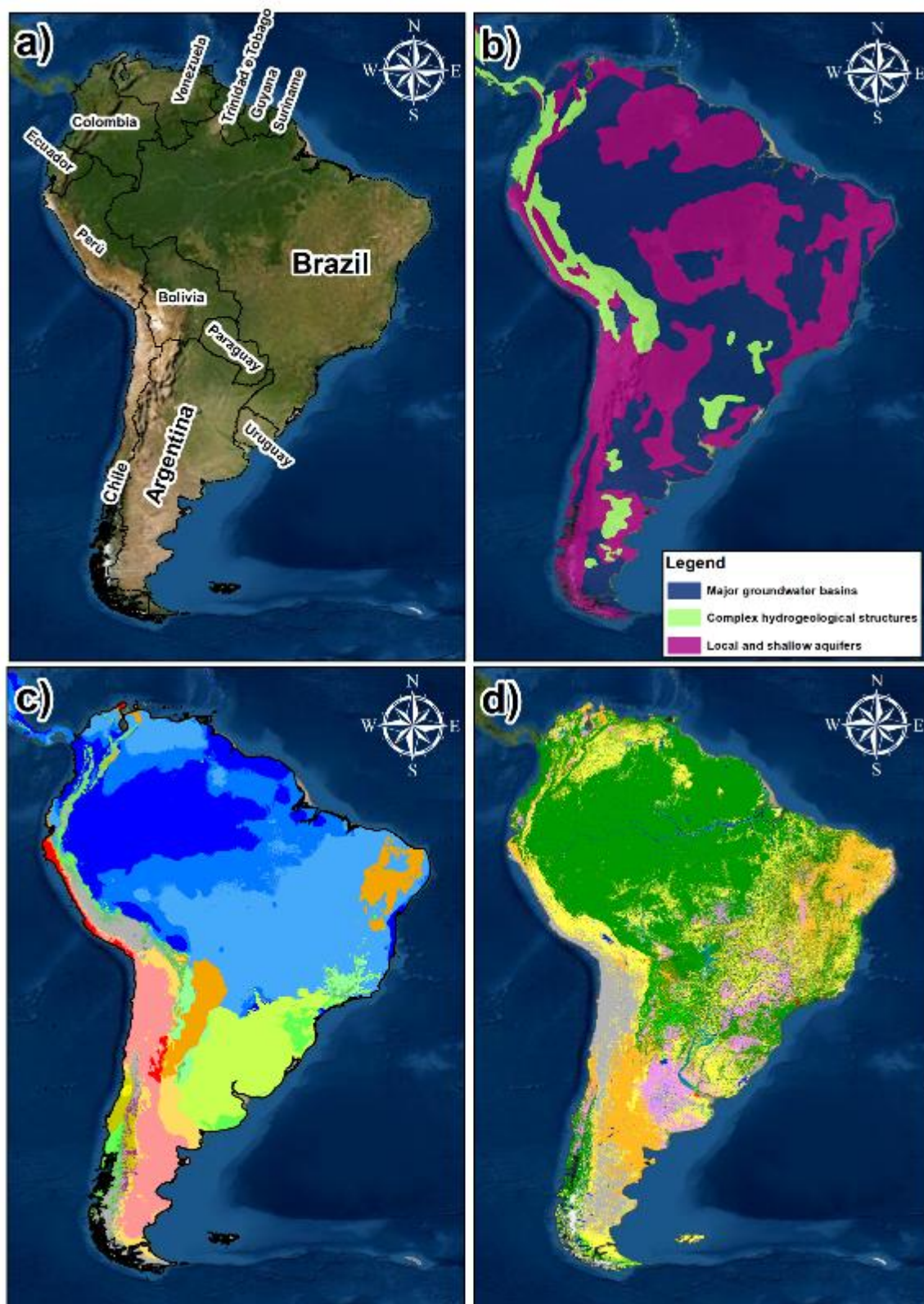


**Fig. 2:** South America overview: a) Administrative limits (ESRI Digital Globe 2021); b) Distribution of groundwater resources (adapted from WHYMAP, Richts et al, 2011); c) Koppen-Geiger climate classification (adapted from Beck et al., 2018); d) Land use as reported in Corine Land Cover (adapted from European Union, Copernicus Land Monitoring Service 2018). Detailed legends for c) Koppen-Geiger climate classification and d) for CLC are available in the Supplementary Material (Fig. S2).

### 3. MATERIALS AND METHODS

#### 3.1. DRASTIC method

DRASTIC is an index and rating method based on the overlapping of a set of factors (i.e. indexes), which represent a synthesis of available information to characterize specific hydrogeological settings in a certain area (Aller et al., 1987). Those settings affect the sensitivity of an aquifer to a potential contamination from the land surface (i.e. intrinsic), but do not take into account specific land uses or chemical characteristics of dissolved compounds (e.g. persistence, mobility, adsorption) required for a risk/hazard assessment (i.e. specific). In DRASTIC, indexes represent Depth to water table (D), net Recharge (R), Aquifer type (A), Soil media (S), Topography (T), Impact of vadose zone (I), and hydraulic Conductivity (C). The method, designed as a linear combination of the ratings of those indexes in every pixel  $i$ , is described by:

$$V_i = D_w * D_{r,i} + R_w * R_{r,i} + A_w * A_{r,i} + S_w * S_{r,i} + T_w * T_{r,i} + I_w * I_{r,i} + C_w * C_{r,i} \quad (1)$$

Where  $V_i$  is the overall DRASTIC score in every pixel  $i$  (i.e. unit grid cell), which represents the intrinsic aquifer vulnerability score in that location.

Theoretically, each index should be an independent variable that describe a specific process or condition related with leaching process in a seven-dimension space. Indexes can be rated from 1 (aquifer not vulnerable to that factor) to 10 (highly vulnerable to that factor) based on specific settings in a certain location (subscript  $r$  in Eq.1). In addition, each index is weighted from 1 to 5 based on its relative importance in the overall leaching process (subscript  $w$  in Eq.1). Consequently, DRASTIC is subject to interpretation and expert judgement in the selection of weighting and rating values of the indexes. More details about the classification of ratings and weights in DRASTIC are available in the supplement (Table S1). DRASTIC scores may range from 23 (minimum vulnerability) to 226 (maximum vulnerability). However, scores close to the minimum and maximum are quite unlikely, as is the occurrence of all highly unfavourable (or favourable) environmental conditions for groundwater leaching in the same place. From a statistical point of view, the population of those scores have a gaussian distribution with most of data assembled around the mean (Fig. S2). Therefore, less than 10% of overall scores would be higher than 160, which is the limit of high vulnerability by Aller et al. (1987). Consequently, to better reproduce the effective vulnerability, many researchers have adapted the limits of the classes according to the distribution of scores in the specific study area. Numerous classifications were proposed, and among those, the geometrical interval is one of the most employed (Kazakis and Voudouris, 2015; Busico et al., 2020). Based on these considerations, the limits of the five vulnerability classes in this paper were based on the analysis of the statistical

267 distribution of DRASTIC scores in South America. Thus, intrinsic aquifer vulnerability is classified  
268 from very low (i.e., scores lower than 90) to very high (scores higher than 180), passing through low  
269 (scores: 90-115), moderate (scores: 115-140), and high vulnerability (scores: 140-180). Using such  
270 limits for the classes allows low (green), medium (yellow) and high (red) scores to be more balanced  
271 in terms of cumulative density function, having ~33% of population in each class (Fig. S2).  
272 Vulnerability classes inform on groundwater protection needs at local scale (Foster et al., 2013) and  
273 can be used to compare those needs between locations in different countries, having a common  
274 conceptual framework developed at continental scale.

275

### 276 **3.2. Data collection and screening of selected datasets**

277 The most important but challenging steps in assessing groundwater vulnerability by index and rating  
278 methods are: i) a comprehensive data collection, ii) a quality control and consistency analysis of input  
279 data, and iii) a data harmonization that focus on granularity of results. In theory, a vulnerability  
280 assessment should rely on robust field data and make use of a comprehensive understanding of natural  
281 processes. In practice, it mostly represents a “best professional synthesis” of already available  
282 information (Foster et al., 2013). This can be satisfactory for local applications since usually datasets  
283 are more detailed and anyway accompanied by field monitoring. For larger scales, where technical  
284 knowledge of field-level conditions decreases and uncertainties/artefacts in datasets increase, an  
285 extended data collection, harmonization and quality control is required to build this professional  
286 synthesis on comprehensive and reliable information. Nowadays, large availability of global datasets  
287 enhances technical possibilities and global applications of methods. However, uncritical uses of  
288 global databases can prove to be erroneous and dangerous in a vulnerability assessment, regardless  
289 of the method chosen. While avoiding looking into artefacts and incongruencies in a global input  
290 layer can produce a visually suitable outcome in terms of mapping, it will also incorporate  
291 inconsistencies and uncertainties in the vulnerability assessment difficult to be isolated in a final  
292 score. The result would be a poor prediction of actual aquifer vulnerability, which is based on local  
293 specific conditions, undermining practical uses of the calibrated assessment. For this reason, the first  
294 phases of a well-conducted vulnerability assessment should entail: (1) gathering as much information  
295 as possible, both globally and locally, (2) checking quality and consistency of data in the specific area  
296 of interest, (3) challenging global data against field measurements (if available), local information  
297 and professional knowledge, and finally (4) integrating and harmonizing datasets with different  
298 spatial resolution/extent or scale. Accordingly, the present work is based on a wide collection of open-  
299 access datasets at different scale (i.e., regional/national/continental/global), processed and spatially  
300 integrated in a GIS environment, cross-checked using location and descriptive attributes from

different sources and technical judgment of local experts. All the maps were rasterized using a fixed 250 m squared pixel as spatial resolution, which results in a cartographic scale of 1:500k (Tobler, 1987). Data sources and data specifications are extensively described in Table S2 and can be accessed by a dedicated repository (Rama et al., 2021).

### 3.3. Sensitivity analysis (SA)

The main drawback of rating methods is their high sensitivity to scores and weights of the indexes, which are essentially subject to a technical judgment of an expert and can be even seen as arbitrary values. For this reason, vulnerability assessments need to objectify and challenge their assumptions with mathematical procedures, such as sensitivity and uncertainty analysis. A sensitivity analysis (SA) helps in addressing the significance of a subjective component, establishing the importance of the weight assigned to a certain parameter. Single parameter SA allows comparing original or “theoretical” weights used in a rating method (Table S1) with effective or actual weights of each parameter computed by the map (Napolitano and Fabbri, 1996). It represents a univariate analysis of the effective weight of each parameter, performed in a spatially variable domain of ratings like a raster map. By following Eq. 2, it is possible to establish in every pixel (i) the effective importance of a single parameter over the overall vulnerability score ( $V_i$ ), rather than the “theoretical” DRASTIC weight by Eq. 3:

$$EW_i = \left( P_{r,i} \times \frac{P_w}{V_i} \right) \quad (2)$$

$$OW = \frac{P_w}{\sum_{j=1}^{n=7} P_{w,j}} \quad (3)$$

where  $EW_i$  is the effective weight of each parameter in every pixel  $i$ ,  $P_{r,i}$  is the rating assigned to an index in a pixel  $i$  (i.e., spatially variable),  $P_w$  is the original weight of this index (i.e., fixed) assigned by the DRASTIC framework, and  $V_i$  is the overall vulnerability score in the DRASTIC map.

Finally, to assess the sensitivity of the DRASTIC score to a single index of the method, a map removal SA was also performed (Lodwick et al. 1990). This map removal is carried out by neglecting a single index in the DRASTIC method and estimating the effect of the removal over the overall score. The method is described by the Eq. 4:

$$S_i = (|V_i/n - V_i'/n'|/V_i) \quad (4)$$

where  $S_i$  is the sensitivity rate, representing the average effect of removing indexes from the methodology,  $V_i$  is the overall DRASTIC score in every pixel  $i$ ,  $V'_i$  is the vulnerability score neglecting the removed indexes,  $n$  and  $n'$  are the number of data layers used to calculate  $V_i$  and  $V'_i$ . Both methodologies have been applied by many authors, alone or in combination, in groundwater vulnerability assessment, seawater intrusion and fire-risk mapping at different scales (Babiker et al., 2005; Huan et al., 2012; Neshat et al., 2014; Kazakis and Voudouris, 2015; Pacheco et al., 2015; Ouedraogo et al., 2016; Busico et al., 2019; Kazakis et al., 2019)

339

### 3.4. Validation of DRASTIC map

Validation is the task of confirming that the outputs of a model are acceptable with respect to an independent set of data that represents a certain mechanism. The validation of a DRASTIC map, representing the intrinsic vulnerability of groundwater across a continent, is a challenging exercise. For this reason, the assessment presented here was validated by checking its accuracy and reliability using different approaches. First, a spatial cross-validation with previous regional vulnerability assessments was performed. The merit of assessments with smaller extension is to be closer to territories and communities, use input data with higher resolution and have a better understanding of natural processes, details, and exceptions. However, local assessments with too small extension (e.g. field or basin) were considered unreliable for a cross-validation of a continental map and for this reason neglected in this study. Therefore, two regional vulnerability assessments in completely different environments were selected for this purpose: the vulnerability map of São Paulo state, Brazil (Hirata et al., 1991) and Rapel district assessment, Chile (Arumi and Jara, 2009). For consistency in the comparison, both maps were developed using the GOD method. Second, a comparison of DRASTIC score versus point measures of groundwater quality was performed. Groundwater concentrations from ~150 wells across Chile (DGA, 2019) and 50 monitoring locations for NO<sub>3</sub><sup>-</sup> in São Paulo state (CETESB, 2021) were used in this step. It is worth stressing that such a comparison of an intrinsic vulnerability map versus point measures is a controversial exercise. Vulnerability maps represent a static picture of the sensitivity of aquifers to vertical leaching through soil and unsaturated zone. Conversely, groundwater concentrations monitored at individual wells can be affected by transport and accumulation, being usually summoned by water withdrawals and drawdown cones (e.g., pumping wells). In addition, multiple measures from wells, even if averaged over time, represent seasonality of subsurface natural processes and anthropic pressure. Therefore, these two kinds of information should be considered complementary rather than interchangeable to achieve a comprehensive assessment of groundwater protection needs. For all these reasons, correlations between concentrations and DRASTIC scores at point level is always very poor (Lasagna et al.,

366 2016). Consequently, to try improving overall correlation with point measures, a normalization with  
367 upgradient distances is proposed. The upgradient distance indicates a linear average space between  
368 the well and the subsurface watershed and may represents an indirect measure of the probability of  
369 collecting solute concentrations from sources located upgradient to the well.

370

#### 371 **4. RESULTS AND DISCUSSION**

372 The development of this first groundwater vulnerability assessment at continental scale for South  
373 America is now introduced. To appreciate all strengths and weaknesses implied in the vulnerability  
374 score, each index of the method is presented and discussed in a dedicated section before introducing  
375 the overall DRASTIC map at continental scale.

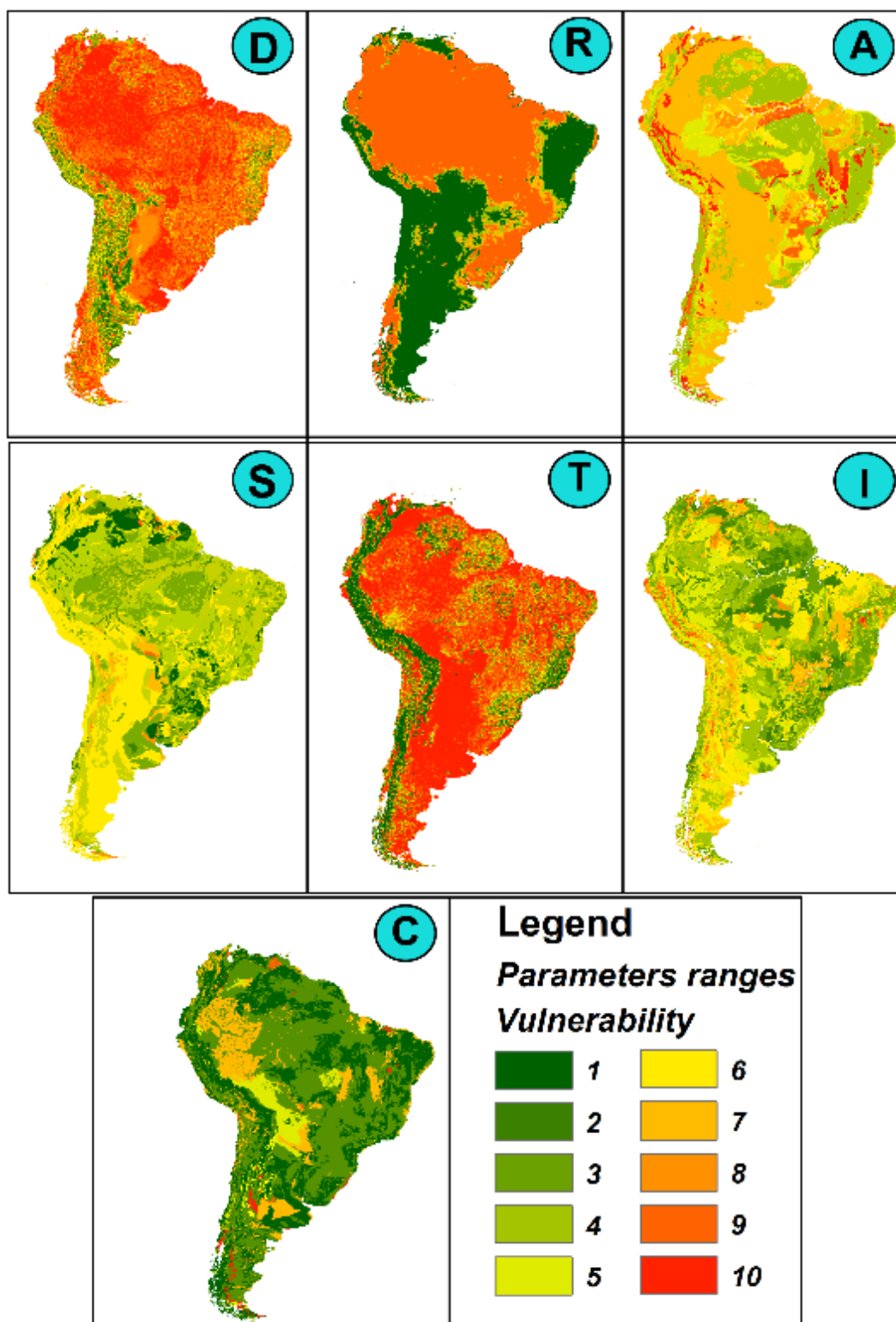


**Fig. 3:** Representation of rating classification of single DRASTIC parameters for South America (based on DRASTIC weights and classes described in Table S1). High-resolution version of those maps is stored in a dedicated repository (Rama et al., 2021).

#### 4.1. Depth to water table (D)

The depth to water table index (D) represents the maximum extent of the leaching process, defining the travel distance (and thereby time) of dissolved pollutants into the vadose zone (Aller et al., 1987).

384 It is based on an average water table position in the pixel (i.e., average hydraulic head of unconfined  
385 aquifer), by considering the aquifer as a steady-state water body. This assumption brings to two major  
386 conceptual limitations: (1) the discontinuity (i.e., averaged over the pixel) and wide range of depths  
387 encompassed in the map, which make difficult to look at the vulnerability as a continuum at  
388 continental scale, and (2) the misrepresentation of transient mixing and vertical flux processes near  
389 the top of the aquifer with a stationary water table. It was demonstrated that water-table fluctuations  
390 increase mass transfer and transport of dissolved compounds by affecting their dissolution, dispersion  
391 and mixing (Goode and Konikow, 1990; Davis et al., 1999; Vanderborght et al., 2000; Dobson et al.,  
392 2007; Rama et al., 2019). However, the major practical issue in including water table fluctuations in  
393 a sort of “transient” D index is given by the absence of those data, especially for large domains.  
394 Accordingly, in this paper, D index relies on a simulated estimation of the stationary water table depth  
395 for South America at ~250 m planar resolution (Fan and Miguez-Macho, 2010; Miguez-Macho and  
396 Fan, 2012a, b), which provide enough granularity to go from regional to local scale. This map,  
397 specific for South America, was preferred to the global outcome at ~1 km resolution (Fan et al., 2013)  
398 and to other outcomes from hydrological models such as PCR-GLOBWB v2.0 (de Graaf et al., 2015;  
399 2019) in reason of its higher resolution. It is worth stressing that the high-resolution depth to water  
400 map has been calibrated and validated using measures of water table coming from more than 30k  
401 monitoring stations located all over the continent (Fan et al., 2013). Based on D ratings, about 60%  
402 of South America is classified as vulnerable for depth to water (Fig. 3), having about 35% of the  
403 continent with very shallow aquifers (<5 m). Next steps of this work would investigate the impact of  
404 water table fluctuations, including transient groundwater levels into the intrinsic vulnerability  
405 assessment, especially in regions with shallow aquifers affected by large water table fluctuations.

406

#### 407 **4.2. Net recharge (R)**

408 The net recharge index (R) in DRASTIC represents water inputs into the aquifer system. Accordingly,  
409 net recharge can be seen as the total quantity of water that reach the aquifer in a certain period,  
410 generally given as a column of water over a year (e.g., mm/y). In this framework, precipitation is  
411 considered as the main driver of leaching, which moves pollutants from topsoil to the aquifer through  
412 infiltration and percolation. Accordingly, a simplistic approach to DRASTIC recharge would only  
413 include precipitation and would neglect any other water input, like irrigation, wastewater, and  
414 artificial recharge (Aller et al., 1987). To tackle this issue, in this paper recharge was estimated from  
415 the subsurface water balance of PCR-GLOBWB v2.0 (Sutanudjaja et al., 2018), a grid-based global  
416 hydrology model able to simulates all water exchanges between soil, atmosphere, and groundwater  
417 reservoirs (Fig. S3). Recharge values come from the outputs of a transient run between 1995-2015,

418 averaged and summed up over time. Therefore, the recharge values used to establish the R index also  
419 include water volumes from irrigation, evapotranspiration, runoff, interflow, and main anthropic  
420 activities. Such numeric outputs were preferred to the recharge estimates from an empirical model  
421 (Mohan et al., 2018), to a direct elaboration of precipitation data from WorldClim v2.1 (Fick and  
422 Hijmans, 2017), and to a simple water balance based on ERA5-Land data from ECMWF web site  
423 (Muñoz-Sabater, 2019), which would have neglected other water inputs into the system. The  
424 classification of R index confirms that highly vulnerable areas for recharge ( $>250$  mm/y) are located  
425 in tropical and subtropical regions of South America (Amazon Forest, Orinoco, and La Plata system),  
426 while less vulnerable areas characterize arid and semi-arid regions like Northern Chile and Northeast  
427 of Brazil (Fig. 3). The major limitation of recharge data is the spatial resolution, having PCR-  
428 GLOBWB v2.0 a computational grid of 5 arcminute ( $\sim 10$  km at the equator). To further improve  
429 spatial resolution and overall accuracy, next steps should investigate other recharge estimates as  
430 inputs for the R index (e.g., outputs from different global models as WaterGAP and H-TESSEL or  
431 approaching other analytical calculation to estimate the recharge). Those products may provide a finer  
432 resolution or a better estimation of recharge fluxes in critical areas, such as dry and wet regions. In  
433 addition, if recharge is the sum of main water inputs in an area, it will progressively change over time,  
434 and is massively affected by human activities. However, this fact clashes with an intrinsic  
435 vulnerability definition, which should neglect anthropogenic activities. For this reason, next steps of  
436 this work would investigate the use of recharge volumes in the definition of pollution loads for a  
437 specific vulnerability assessment. Finally, it is worth stressing that linear relation of recharge and  
438 score in DRASTIC neglects dilution as a possible mechanism reducing aquifer vulnerability in areas  
439 with massive precipitation. This assumption was maintained in the present work as worst-case  
440 scenario, but authors would recommend adopting a more physically based description of vulnerability  
441 by recharge that includes dilution, as for example is done in SINTACS methodology (Civita and De  
442 Maio, 2004).

443

#### 444 **4.3. Aquifer type (A)**

445 The aquifer index (A) describes unconsolidated deposits and consolidated lithology that host the  
446 aquifer itself and may affect with their characteristics the local flow system. Once dissolved  
447 compounds have reached the saturated zone, the residual attenuation capacity of subsurface system  
448 is related with four main mechanisms: i) dispersion, ii) dilution, iii) absorption, and iv) chemical  
449 reactivity of the media. Being mostly affected by tortuosity of filtration paths (i.e. travel length and  
450 time), those processes are summarized through the geological characteristics of media, ranging from  
451 less sensitive formations (e.g. shale and metamorphic rock) to most vulnerable ones (e.g. karst and

coarse unconsolidated environments) (Table S1). In this work A index was obtained by integrating a continental geological map of South America at 1:5M (Gómez et al., 2019) with more detailed hydrogeological datasets of Brazil, Chile, and Argentina (Table S2). Different layers were combined in a new one using spatial analysis tools in GIS, achieving local enhancements of spatial discretization. Geologically, whole continent was divided in seven main domains (i.e. Sedimentary, Porous/Fissured, Carbonates, Crystalline, Volcanic, Metamorphic, and Cenozoic). The vulnerability of each feature was classified by the information on its geological domain, aquifer type (i.e. karst, fissured/fractured, porous, mixed), degree of fractures (i.e. no, low, medium, high), aquifer productivity (i.e. non-productive, extremely low, low, medium, and high) and transmissivity (with K ranging from  $>E-4$  to  $<E-8$ ). The highest vulnerability (ratings 9-10) to “aquifer type” was assigned to karst environments and very conductive porous media like main river valleys and coastal areas, while non-productive volcanic and crystalline bedrocks received the lowest ratings 2-3. A rate of 5 to 6 were instead assigned to fractured and metamorphic formation outcropping in Brazil and Argentina (Fig. 3).

466

#### 4.4 Soil attenuation (S)

The soil index (S) accounts for the attenuation capacity of topsoil media in the leaching process. Soil is the upper layer of the vadose zone, more organic and weathered, characterized by an intense biological activity, which represents the initial natural barrier to the pollutant infiltration (Aller et al., 1987). In DRASTIC, all attenuation mechanisms that may depend on soil properties (e.g., biodegradation, adsorption, fixation) are summarized by the USDA textural class, which only depends on percent content of silt, clay, and sand. Accordingly, fine materials (e.g., clay and silt), which are less permeable, are classified as less vulnerable than coarse textures (e.g., sand and gravel) that allows a more rapid infiltration. This assumption entails a homogeneous medium and a uniform chromatographic flow in the column, and completely overlooks anisotropies (e.g., root and earthworm channels, fissures and interaggregate voids) that usually drive non-equilibrium water flow in the first 50-100 cm of soil. It is worth stressing that this simplification of soil complexity can bring in some cases to a misrepresentation of infiltration, as it happens for heavy/aggregated soils where bypass flow and preferential pathways can control the leaching process (Jarvis, 2007; van der Heijden et al., 2013). However, by looking processes on average over extended areas (i.e., 250 m pixel), a chromatographic flow controlled by main textural class still seems to be a reasonable representation of infiltration through the soil column, since at larger scales the preferential pathways effects are usually mediated while other features like surface depressions, faults and discontinuous layers prevail (Hendrickx and Flury, 2001). In this paper, S index was defined by combining datasets with different

spatial extent (Table S2). A preliminary distribution of soil texture for the continent was defined with the Harmonized World Soil database (FAO, 2012), a vectorial geodatabase obtained from a 30'' resolution map. The distribution was refined using 3,000 soil columns from World Soil Information Service (Batjes et al., 2020). Finally, information from two extensive databases at national scale as HYBRAS (Ottoni et al., 2018) and PRONASOLOS (Cooper et al., 2005) allowed a more detailed discretization of topsoil properties in Brazil with more than 30,000 soils profiles. Dominant soil textures at continental scale are loams, suggesting a relative low vulnerability to leaching (ratings 2-6) in most of South America (Fig. 3).

494

#### 4.5 Slope or topography (T)

The topography index (T) accounts for the impact of land surface onto the leaching mechanism. In terms of water balance, precipitation generates three fluxes (i.e., runoff, recharge, evapotranspiration), whose equilibrium is controlled by local conditions of climate, topography, and hydrogeology. Therefore, topography index would represent a qualitative indication of the ratio of runoff to infiltration based on terrain's slope only. Unlike more recent "overlay and index" methods designed for karst (e.g., COP and PaPRIKa), T index in DRASTIC neglects any interaction of topography with other surface features (e.g., hydrology network, colluvial deposits, sinkholes) or geology (e.g., impervious formations). For this reason, it should be considered as a simple indication of terrain slope, rather than a sophisticated link between topography and infiltration. In this work, surface slope was estimated in a GIS environment from MERIT DEM, which is an unbiased ~90 m resolution global map of terrain elevation (Table S2). It was developed using existing spaceborne DEMs as SRTM3 v2.1 and AW3D-30m v1, by removing multiple error components such as absolute bias, stripe noise, speckle noise, and tree height bias (Yamazaki et al., 2017). A clear gap is shown in the classification of T index (Fig. 3) between flat morphology (0–4%) that dominates major river valleys and large continental flatlands (ratings 9-10), and steep geography that characterizes Andean regions along the Pacific coast (ratings 1-2).

512

#### 4.6 Impact of vadose zone (I)

The index I aims to estimate the attenuation capacity afforded by unsaturated zone, which lays between the topsoil and the aquifer (or, more precisely, the top of capillary fringe). Unfortunately, spatial information and global datasets characterizing this zone are rare and generally scattered. For example, only few databases provide consistent information of lithology depth, differentiating surficial and deep deposits. Therefore, to address I index is common interpolating more widely available data of topsoil and aquifers. In this paper, the impact of vadose zone was based on the ratio

of depth-to-bedrock (DTB) (Shangguan et al., 2017) to depth-to-water (DTW) (Fan et al., 2013), following Eq. 5 (map showed in supplement, Fig. S4):

$$I = \begin{cases} 0 & \text{IF } (DTW < DTB) \\ 1 + \frac{DTB}{DTW} & \text{IF } (DTB \geq DTB) \end{cases} \quad (5)$$

The ratio represents the percentage importance of unconsolidated materials and deep lithologies on the characteristics of vadose zone, and thereby, the classification of I index. Accordingly, a value close to 1 (i.e.,  $DTW \gg DTB$ ) would indicate an aquifer hosted in deep lithological materials and a little importance of unconsolidated deposits, while a value close to 2 (i.e.,  $DTW \sim DTB$ ) would suggest a major impact of unconsolidated materials on overall vadose zone. Conversely, a value of 0 would represent a water table hosted in the unconsolidated materials, having a vadose zone only affected by the characteristics of those deposits. Information about unconsolidated deposits were obtained from a global high-resolution dataset of soil parameters, 1-3 m deep (Dai et al., 2019). The USDA textural class is estimated first, by the percentage content of sand-clay-silt, and then information on coarse deposits (e.g., gravel) and organic matter (e.g., peat and muck) is added (Fig. S5). For deep lithologies, already available geological data were used, as presented in Section 4.3 (A index). An in-depth description of all employed datasets is available in Table S2. The resulting map of I index (Fig. 3) confirms that most of South America have low to medium vulnerability geological media, as already anticipated by A and S indexes.

#### 4.7 Hydraulic conductivity (C)

The index C represents the ability of the aquifer itself to transmit water, and thereby, how water will flow under the land surface where the vulnerability is assessed. Accordingly, this factor will ultimately summarize the rate at which contaminant move away from the infiltration point. It is based on horizontal hydraulic conductivity of the saturated zone (Ks). In this work, C index was estimated combining two versions of a global dataset of log permeabilities (GLHYMPS v1.0 and v2.0) (Gleeson et al., 2014; Huscroft et al., 2018), whose characteristics were summarized in Table S2. To use those data, a prior quality check of spatial consistency was performed. Data were checked against geological and hydrogeological maps (Gómez et al., 2019; CPRM website), removing boundary artefacts, fixing spatial discrepancies, and even reshaping polygons on the borders to match the permeability map with the underneath geological map. The Ks information was also challenged against the description of deposits (i.e., information stored in datasets at national level) and fixed if they were not consistent (e.g., same deposits having different hydraulic conductivity on different sides

of a national border). It is worth remembering that global datasets are powerful sources of data for risk assessments. However, they can include artefacts and spatial discrepancies (especially on the national borders), unavoidably coming from complex integration of different data sources in different languages. Such discrepancies are though extremely relevant for a local vulnerability assessment and need to be (manually) fixed and double-checked with local experts before using such layers. Overall, classification of C index did not show a wide variability of ratings across the continent, being most of the territory characterized by Ks of 0.1 to 10 m/d (ratings 1-2) and having less than 20% of aquifers a Ks greater than 10 m/d (Fig. 3).

562

#### 563 **4.8 Intrinsic aquifer vulnerability: map of DRASTIC score**

564 The intrinsic aquifer vulnerability of South America was estimated by DRASTIC (Fig 4), combining  
565 seven relevant indexes (Fig. 3) through a linear combination (Eq.1). Obtained scores in the map  
566 ranged from 35 to 212. They were classified in 5 classes of vulnerability from very low (dark green)  
567 to very high (red) using intervals described in the methodology (Section 3.1).

568

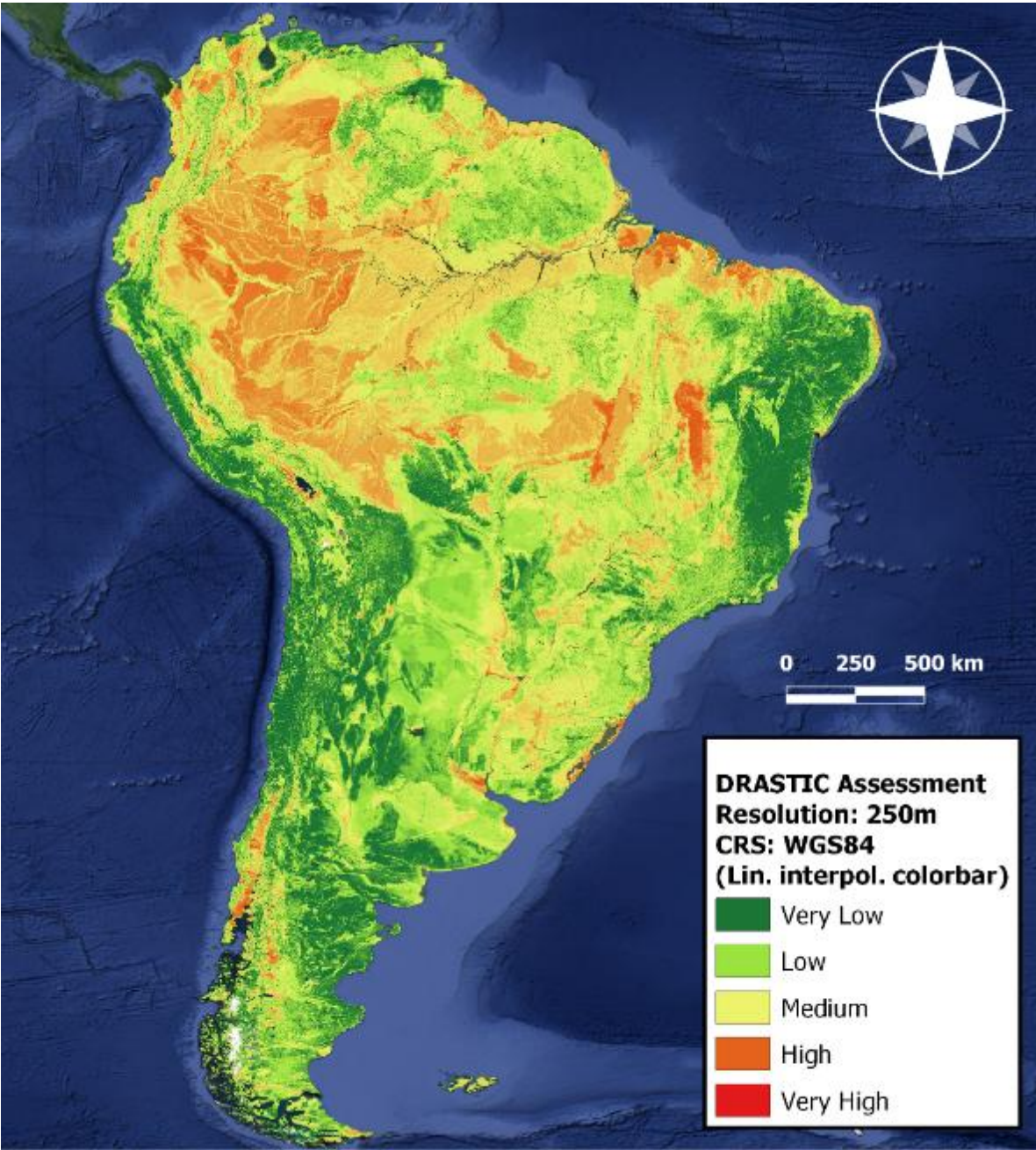
569 **Table 1:** Summary of main statistics of DRASTIC indexes.

Parameter	Min	Max	Mean	St.Dev.	CV (%)
<b>D</b>	1	10	7.86	2.50	31.81
<b>R</b>	1	9	5.48	3.84	70.07
<b>A</b>	3	10	5.85	2.05	35.04
<b>S</b>	1	9	4.52	1.56	34.51
<b>T</b>	1	10	7.58	3.19	42.08
<b>I</b>	1	10	4.62	1.64	35.50
<b>C</b>	1	10	2.74	2.41	87.96

570

571 The main statistics of the seven hydrogeological factors are shown in Table 1. Indexes D and T present  
572 the highest mean values (i.e. 7.86 and 7.58, respectively), which are driven by the typical  
573 characteristics of the continent: large basins with shallow aquifers and extensive regions with plateaus  
574 and plains (see Section 2 for more details). On the other hand, indexes C and R show higher  
575 coefficient of variation (CV) than the other parameters (i.e. 87.96 and 70.07%, respectively).  
576 Statistically, the CV represents the extent of variability in relation to the mean of the population,  
577 which indicates a high spatial variability of the ratings of those indexes across the continent (Vu et  
578 al., 2019). A simplified representation of each index is given in a ridgeline plot (Fig. 5a), where is  
579 possible to appreciate, graphically, the previous assumptions by a summary of the distribution of  
580 about 1M pixels in each raster. In addition, a detailed histogram (bin width=1) shows the probability  
581 density function of final DRASTIC scores in South America (Fig. 5b), underlining the proposed

582 classification of vulnerabilities. The graphical outcome has a pixel dimension of 250 m and a  
583 cartography scale of 1:500k. However, it should not be inferred that intrinsic vulnerability has been  
584 strictly mapped to this precision in all the continent, having some of the inputs a coarser resolution,  
585 even after combining local and international datasets.  
586



587  
588 **Fig. 4:** Intrinsic aquifer vulnerability map of South America based on a DRASTIC assessment (Base map from  
589 © Google Satellite 2021). High-resolution version of this raster is available on a dedicated repository (Rama  
590 et al., 2021).  
591

592 The results indicate that most of the continent has a very low to moderate intrinsic vulnerability  
593 (~70%), probably due to quite deep aquifers, very rich/heavy soils and extended areas with surficial

crystalline formations that may prevent infiltration. About 10% of the continent shows a very low vulnerability (dark green), which suggests the concurrent presence of hydrogeological conditions that favour the attenuation capacity in at least 4-5 indexes. For example, Atacama region (North Chile/Argentina and South Peru) presents very low to low vulnerability driven by very deep aquifers and very low precipitation per year, despite a quite permeable soil/subsurface system. Exceptions to this low vulnerability trend are represented by alluvial valleys of major rivers, continental aeolian sands, sandy areas near the coast, or rainy valleys with colluvial deposits in Andean Cordillera. Those regions show high or very high aquifer vulnerability (in total about 30% of the territory), having hydrogeological settings that drive a fast infiltration of high rainfall volumes. However, only a small part of the continent (i.e. about 0.6%) presents DRASTIC scores higher than 180, with only 0.0015% of the pixels having more than 200.

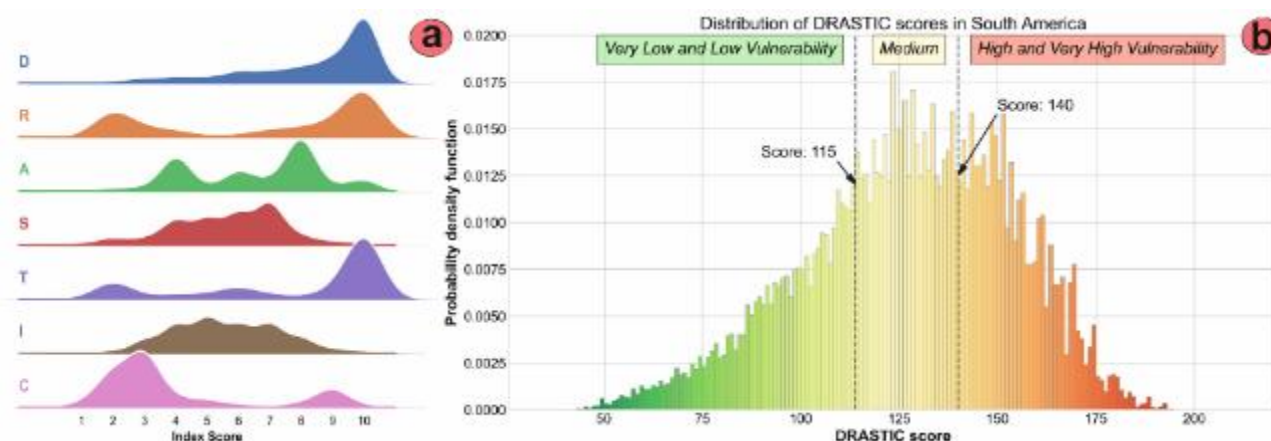
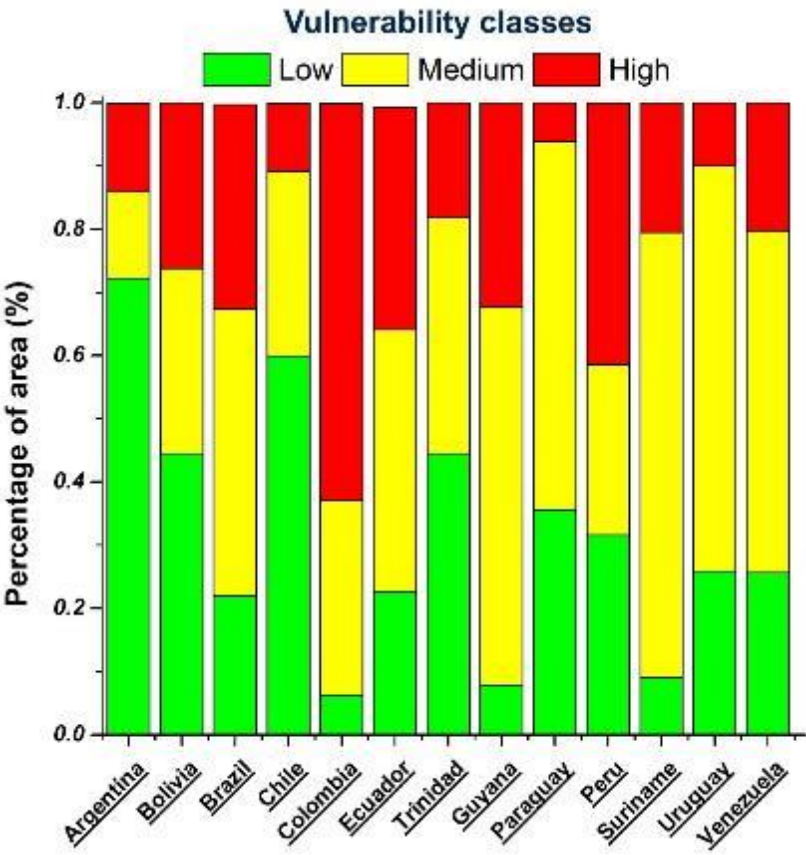


**Fig. 5:** Distribution of scores in single indexes and proposed DRASTIC map. (a) Ridgeline plot of the indexes showing their simplified distribution. (b) Probability density function of DRASTIC scores in South America, showing the limits of adopted vulnerability classes.

It is worth underlining that within a DRASTIC framework, Amazon area (i.e., equatorial climate) would present a higher vulnerability compared to dry regions (e.g., Northeast Brazil, Southwest Bolivia, North Chile), because of its higher cumulated precipitation across the year and regardless of local hydrogeological setting. However, due to the flat topography, small depth to water table, and quite permeable deposits, Amazon aquifers seem to be among the most sensitive to anthropic pollutants in the whole South America. Similarly, valuable aquifers in tropical regions of Colombia are classified as highly vulnerable as Amazon aquifers. Finally, other highly vulnerable areas are found in central/South Chile driven by the low depth to water table and the high Ks of colluvial deposits present in the valleys of the Southern Andean Cordillera.

620 In addition, given the high spatial resolution of DRASTIC map, it was possible to address the  
 621 percentage of aquifer vulnerability classes in each country (Fig. 6). The analysis was performed by a  
 622 spatial analysis in GIS, summarizing the initial five classes of vulnerability into three classes: low  
 623 (by combining very low and low), medium, and high (by combining high and very high). As  
 624 mentioned, hydrogeological settings and environmental conditions of Amazon Forest results in  
 625 intrinsically more vulnerable aquifers in those regions. Consequently, countries with extended  
 626 regions of Amazon rainforest showed wider vulnerable groundwater resources, in order: Colombia  
 627 (63%), Peru (41%), Ecuador (35%), Guyana (32%), and Brazil (32%). In those regions, a strong land  
 628 use change at the expense of rainforest coverage may lead to a fast degradation of groundwater  
 629 resources. Conversely, most extended areas with low vulnerability are concentrated in Argentina  
 630 (72%), Chile (60%), and Bolivia (45%) due to their arid climate and deep aquifer systems.



631  
 632 **Fig. 6:** Stacked bar chart of intrinsic vulnerability classes in each country of South America.  
 633

634 **4.9 Sensitivity analysis**

635 A map removal SA was performed by neglecting a single index per time from DRASTIC, and  
 636 accounting for its effect on the overall score. A summary of the main statistics from the analysis is  
 637 presented on Table 2. The D index shows far the highest impact on the DRASTIC score, both on  
 638 average across the continent (i.e. mean 2.7% and median 2.9%) and locally in certain regions of the

map (i.e. maximum value 13.9%). As expected, the second most important index was R. Conversely, index A and I showed high local impacts on the vulnerability score (max: 4.66% and 6.78%, respectively) but quite low effect on average (mean: 0.66% and 1.16%, respectively). This may be caused by a statistical concurrency of high and low ratings of those indexes across the map, which would result on average in a small effect over the vulnerability score of the continent.

**Table 2:** Summary of main statistics of the map removal sensitivity analysis.

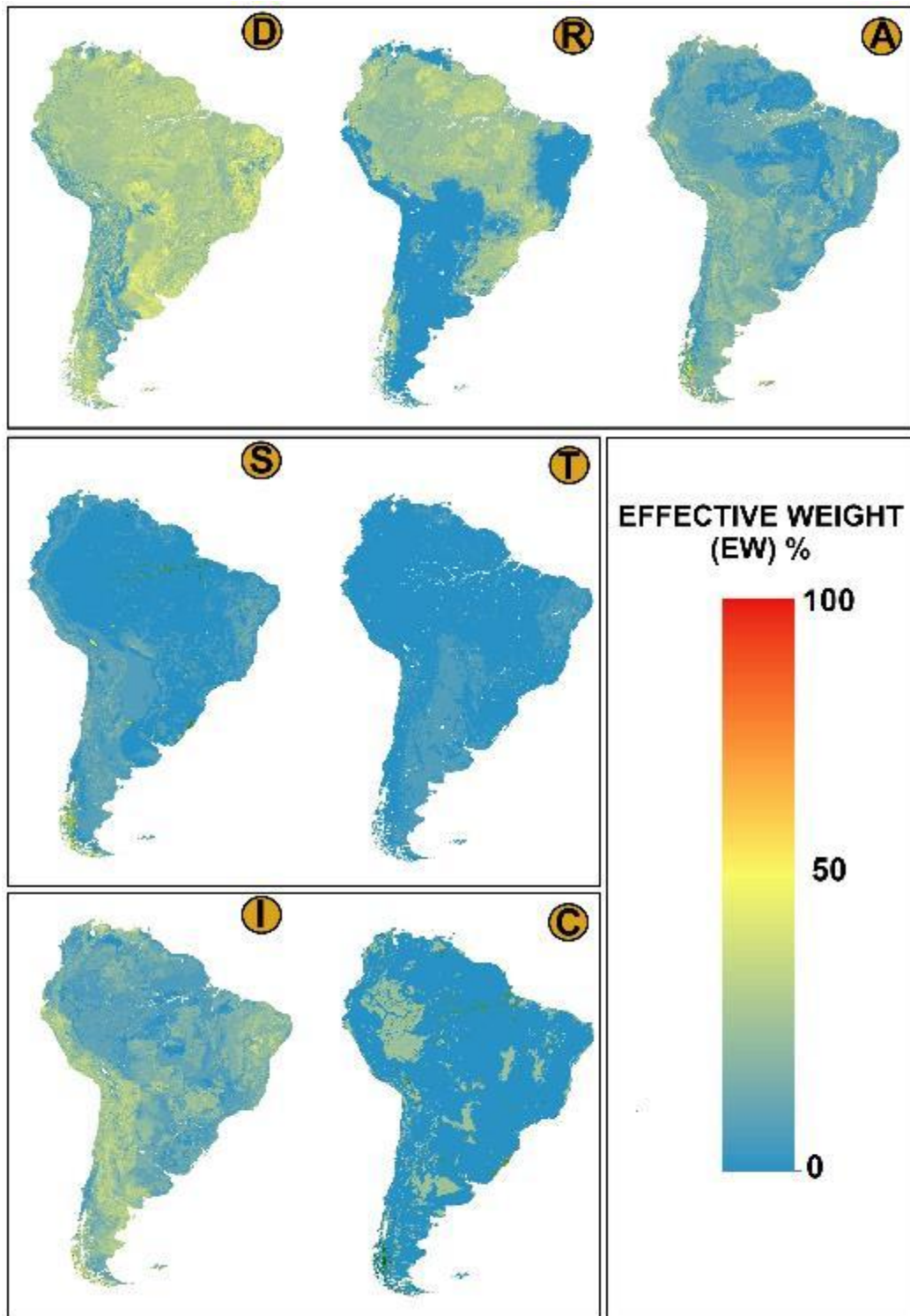
Removed Index	Included Indexes	Sensitivity rate (Si) [%]				
		Mean	Median	SD	Min	Max
<b>D</b>	RASTIC	2.72	2.93	1.37	0.00	13.91
<b>R</b>	DASTIC	1.75	1.76	0.62	0.00	6.07
<b>A</b>	DRSTIC	0.66	0.59	0.47	0.00	4.66
<b>S</b>	DRATIC	1.15	1.21	0.52	0.00	3.50
<b>T</b>	DRASIC	1.37	1.31	0.45	0.00	2.30
<b>I</b>	DRASTC	1.16	0.92	0.99	0.00	6.78
<b>C</b>	DRASTI	1.46	1.64	0.57	0.00	4.76

A single parameters SA was also applied to assess the effectiveness of index weights (EW) within the DRASTIC application in South America. The main outcomes of this analysis are summarised in Table 3. They indicate that most of variability is driven by only four indexes: D (depth-to-water), R (recharge), A (aquifer type), and I (vadose zone media). In the proposed DRASTIC map, on average, these four parameters together have an effective weight of 81%. The results remarked the importance of water inputs (i.e., recharge), travel distance (i.e., depth to water table) and hydrogeological characteristics of crossed media (i.e., aquifer type and vadose zone) in defining the overall attenuation capacity, and consequently, the intrinsic groundwater vulnerability in a specific location.

**Table 3:** Summary of theoretical and effective weight obtained (on average) from a single parameter sensitivity analysis of DRASTIC indexes in South America.

Indexes	P <sub>w</sub> - Original weight by DRASTIC	OW - Theoretical weight by DRASTIC (%)	EW – Effective weight by SA (%)
<b>D</b>	5	21.74	30.61
<b>R</b>	4	17.39	16.29
<b>A</b>	3	13.04	14.08
<b>S</b>	2	8.7	7.62
<b>T</b>	1	4.35	6.04
<b>I</b>	5	21.74	19.12
<b>C</b>	3	13.04	6.32

659 However, depth-to-water (D) was the only parameter in showing a relevant positive increase of its  
660 weight from theoretical to effective ( $\sim 9\%$ ). This entails that not only it is on average the most  
661 important parameter to define by DRASTIC the intrinsic aquifer vulnerability of South America, but  
662 also that its contribution is more important in regions where, due to the low ratings of other indexes,  
663 it ends up making a difference in the overall vulnerability score. At the end, D index alone affects the  
664 vulnerability score by over 30% on average. Conversely, hydraulic conductivity (C) showed a clear  
665 drop in its importance over the DRASTIC score ( $\sim -7\%$ ) driven by an unfavourable distribution of its  
666 low ratings across the map. This fact seems confirming an arithmetical intuition coming from the  
667 ridgeline plot (Fig. 5a): only parameters with positively unbalanced distributions (i.e. centred on high  
668 ratings), like D, T and A, increased their weight in the sensitivity analysis, as opposed to negatively  
669 unbalanced distributions (e.g. C index) that decrease their importance in the analysis. However, most  
670 of the indexes (e.g. R, A, S, T, I) showed no significant variations in their weight, having a  
671 difference between theoretical and effective of about 1-2% (Table 3). Overall, both map removal and  
672 single parameter SA underlined the importance of depth-to-water (D) over the intrinsic vulnerability  
673 assessment of South America by DRASTIC. This index is followed in terms of importance by  
674 recharge (R), which impacts regions with high vulnerability across the continent, and hydraulic  
675 conductivity (C), which affects most regions with low DRASTIC scores. In addition, spatial  
676 variability of the effective weight of the indexes is mapped across the continent (Fig. 7), allowing to  
677 check which parameters matter most in each region. The maps confirm the same trend of average  
678 analysis, with D, R, I, and A having the highest effective weights. Interestingly, regions with high  
679 hydraulic conductivity show that C index had an important impact there over the DRASTIC score.  
680



681

682 **Fig. 7:** Spatial distribution of  $EW_i$  (i.e. effective weight of indexes over the DRASTIC score), assessed by  
 683 single parameter SA and given as a percentage. High-resolution version of those maps is available on a  
 684 dedicated repository (Rama et al., 2021).

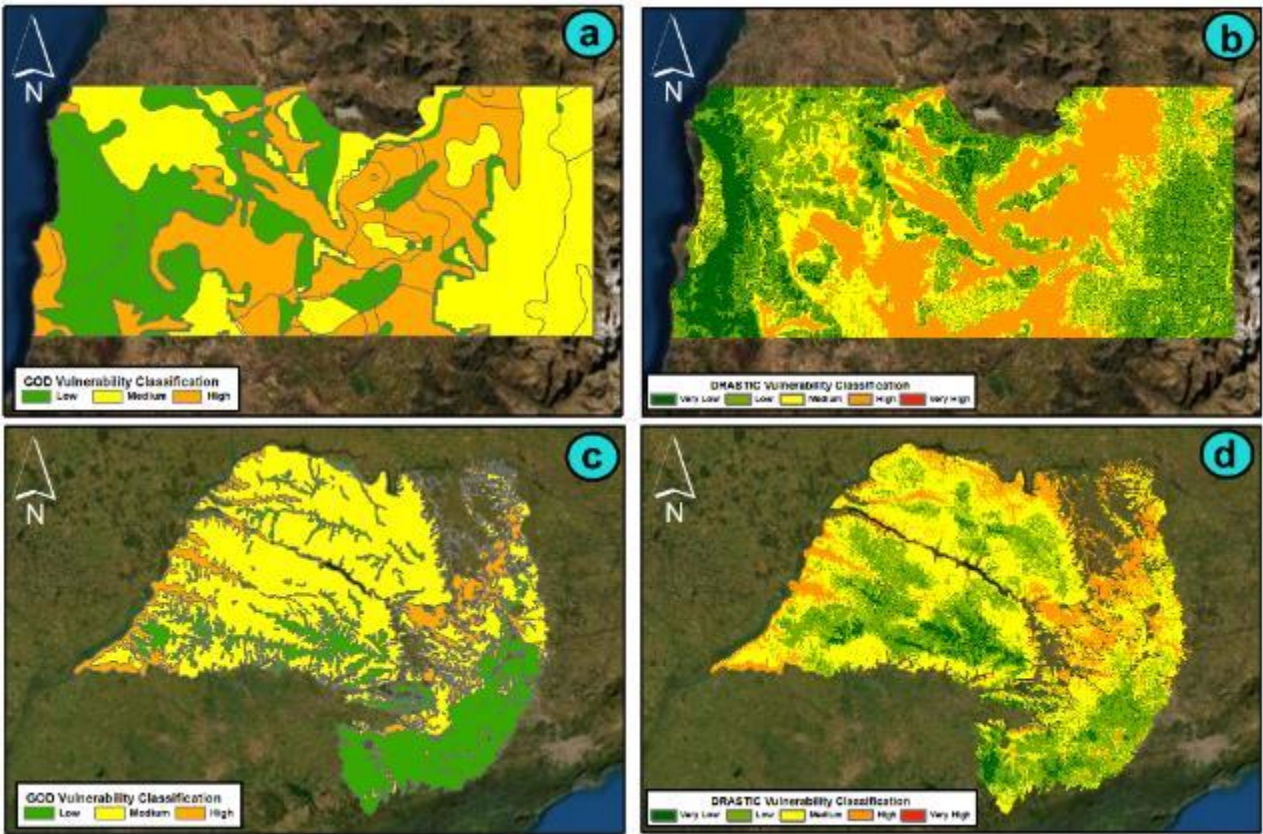
685

686 It is worth underlining that the outcomes may have been partially influenced by the original spatial  
 687 discretization of input files. By excluding R index, which come from model outputs on a regular grid  
 688 (~10 km), there is a strong difference between parameters rasterized from maps/polygons at coarser  
 689 scale (i.e., A, S, I, and C) and indexes estimated from high resolution raster (i.e., D and T). First type

690 includes intrinsically less variability than the latter one, in terms of details and spatial discretization.  
691 High resolution maps allow to spatially define relevant features with extreme conditions (e.g., very  
692 high or very low vulnerability of certain features), as opposite to polygons at greater scale, which  
693 present average values over very large areas (i.e., no extremes). This fact may represent also a limit  
694 to the actual granularity of results in the final map, having three out of the four most important indexes  
695 in terms of effective weight with a limited spatial resolution (i.e. A, R, I).

696  
697 **4.10. Map validation and discussion**

698 The main outcomes of spatial cross-validation showed a good visual agreement between DRASTIC  
699 map of South America and previous regional assessments (Fig. 8). The two regional GOD-based  
700 assessments of Rapel, Chile (Arumi and Jara, 2009) and Sao Paulo district, Brazil (Hirata et al., 1991)  
701 were compared with the DRASTIC-based map at continental scale to check overall consistency and  
702 point out differences.



703  
704 **Fig. 8:** Spatial cross-validation of DRASTIC map: a) GOD-based vulnerability assessment at Rapel district,  
705 Chile (Arumi and Jara, 2009); b) Aquifer vulnerability map of Rapel extracted from the present DRASTIC-  
706 based assessment of South America; c) GOD-based vulnerability assessment of São Paulo state, Brazil (Hirata  
707 et al., 1991); d) Aquifer vulnerability map of São Paulo extracted from the present DRASTIC-based assessment  
708 of South America. Base maps from ESRI Digital Globe 2021.

709

710 In Chile, the assessments with GOD (Fig. 8a) and DRASTIC (Fig. 8b) shows a comparable  
711 classification pattern, highlighting almost the same areas with high and low vulnerability. Especially  
712 highly vulnerable areas seem to be quite consistent each other. Conversely, definition of vulnerability  
713 seems to be more uncertain in the mountain area of the region (i.e., far right side of the domain),  
714 where DRASTIC assessment identified less vulnerable aquifers and GOD classified them with  
715 moderate vulnerability. In Brazil, also, the two maps show a very consistent visual pattern. In the São  
716 Paulo state, GOD (Fig. 8c) and DRASTIC (Fig. 8d) classifications point out highly vulnerable areas  
717 (orange) mainly adjacent to surface water bodies and low vulnerabilities (green) in regions with heavy  
718 soils and low conductive deposits. In both regions, the worst spatial correspondence was found within  
719 the medium vulnerability class, which characterizes a relevant portion of GOD maps. It is worth  
720 underlining that poor discretization of moderate vulnerability is a common and well-known drawback  
721 of index methods (Hu et al., 2018; Kazakis et al., 2019). For this reason, to avoid an oversized area  
722 with moderate vulnerability, the present DRASTIC assessment of South America proposed a  
723 different, domain-specific, set of limits for vulnerability classes. Accordingly, DRASTIC maps in  
724 those two regions showed smaller medium vulnerability areas compared to the GOD ones. To try to  
725 quantify this spatial validation, a simple statistical analysis of DRASTIC scores within the areas  
726 defined by the three vulnerability classes in GOD was also performed (Table 4). Values represent the  
727 average, minimum and maximum DRASTIC score within the green (i.e. low vulnerability), yellow  
728 (i.e. medium vulnerability), and red (i.e. high vulnerability) regions of the GOD assessments (Fig. 8a  
729 and 8c). Results show to be consistent with visual assessment, having for both regions that DRASTIC  
730 scores are considerably increasing from low to high, and its mean falls in the same class of  
731 vulnerability as in GOD. Therefore, average DRASTIC scores within low vulnerability areas in GOD  
732 resulted 105.1 and 101.5, in Sao Paulo and Rapel respectively, which is consistently lower than the  
733 average DRASTIC score in high vulnerability areas (146.5 and 142.8, respectively). In addition, the  
734 overlapping areas with the same vulnerability classes in GOD and DRASTIC were estimated by a  
735 spatial analysis in a GIS environment and summarized in supplementary material (Table S3). For  
736 consistency, very low and low vulnerabilities in DRASTIC were compared with low/negligible  
737 vulnerability in GOD, as well as high and very high classes in DRASTIC were represented by high  
738 vulnerability in GOD. Spatial agreement among low vulnerabilities within the two methods was 70-  
739 75% in the two regions. Similarly, the spatial overlapping of high vulnerabilities on the two regions  
740 ranged between 70 and 85%.

741 **Table 4:** Statistics of DRASTIC scores in areas of low, medium, and high vulnerability from previous  
742 assessments (GOD).

<b>Sao Paulo (Brazil)</b>	<b>LOW VULNERAB. AREAS (GOD)</b>	<b>MEDIUM VULNERAB. AREAS (GOD)</b>	<b>HIGH VULNERAB. AREAS (GOD)</b>
<b>DRASTIC Mean</b>	105.1	119.8	146.5
<b>DRASTIC Min</b>	56.0	62.2	89.2
<b>DRASTIC Max</b>	171.3	178.9	184.8
<b>Rapel (Chile)</b>	<b>LOW VULNERAB. AREAS (GOD)</b>	<b>MEDIUM VULNERAB. AREAS (GOD)</b>	<b>HIGH VULNERAB. AREAS (GOD)</b>
<b>DRASTIC Mean</b>	101.5	115.9	142.8
<b>DRASTIC Min</b>	58.8	69.7	81.7
<b>DRASTIC Max</b>	149.2	160.8	173.3

743

744 Finally, a point comparison between groundwater concentration of target compounds and intrinsic  
745 vulnerability was performed. In Chile, statistically representative values from ~150 wells were plotted  
746 versus DRASTIC scores in the same locations. As expected, a generally poor correlation (mainly  
747 negative) was found between most of the data (Fig. S6 – Graphs at row 1 and 3). However, the  
748 correlation increases drastically by normalizing raw groundwater concentrations with upgradient  
749 distance within the basin (Fig. S6 – Graphs at row 2 and 4). This quantity normalizes the absolute  
750 concentrations in an individual point with the probability to have been transported there from  
751 somewhere else rather than infiltrate by leaching. The more the distance from basin watershed, the  
752 more the chance to receive upgradient contamination affecting that measure. For the São Paulo state,  
753 a satisfactory agreement among NO<sub>3</sub><sup>-</sup> concentrations and final DRASTIC classification was also  
754 found, having in general higher groundwater concentration in areas of more pronounced vulnerability  
755 (Fig. S7).

756

## 757 5. CONCLUSIONS

758 Assessing aquifer vulnerability world-wide is progressively becoming an essential screening tool to  
759 achieve a sustainable management of groundwater resources. This exercise is strictly related with the  
760 Sustainable Development Goals (SDGs) to be achieved by 2030, especially with targets: 6.3 “Improve  
761 water quality by reducing pollution”, 6.5 “Implement integrated water resources management”, and  
762 6.6 “Protect and restore water-related ecosystems”. This is the first time that the intrinsic groundwater  
763 vulnerability of South America has been mapped at continental scale employing an index and rating  
764 methodology (i.e. DRASTIC). The assessment represents the comparative sensitivity of aquifers in  
765 South America to leaching of compounds from the land surface. The proposed map divides the

continent in five classes of vulnerability going from very low to very high, with a general trend of medium to low vulnerability. In many regions, this tendency seems to be driven by deep groundwater, low recharge (e.g., infrequent precipitation) and not much hydraulically conductive deposits (e.g., rich soils, crystalline formations, high clay content). Conversely, alluvial valleys along main rivers and coastal aquifers, which are characterized by shallow groundwater in coarse sediment and high recharge from precipitation, showed a high vulnerability. Both sensitivity analyses (i.e. map removal and single parameter) confirmed the major influence of depth-to-water (D index) on the final DRASTIC score. However, also recharge (R) and hydraulic conductivity (C) showed to have an impact on the assessment of groundwater vulnerability in South America. The cross-validation of the map in two different environmental settings at regional scale (i.e. Rapel, Chile and São Paulo, Brazil) gave satisfactory results with a good agreement between previous and current assessments. To achieve consistent results, a great deal of effort was put into control, collection, and integration of data from international and local databases with different spatial resolution. Data were managed in a GIS environment, which provides an effective tool for handling large amounts of spatial data with different datums, scales, and geometries. Accordingly, the use of international datasets of "open data" should be fostered in this kind of applications as they enable a "pre-screening" of the vulnerability even in regions with sparse and scattered information. Although open datasets would always require an initial quality check to be used, which challenges the reliability and robustness of values themselves, they represent a valuable resource for environmental and geo- scientists. In addition, the present application highlighted the importance of developing a common conceptual framework for the aquifer vulnerability at a transboundary (and even global) scale, applicable in many different hydrogeological settings (e.g. porous, karst, fissured). Thus, possible next steps of this study would be to work towards the development of this common framework at global scale, which potentially may include a broader set of mechanisms of environmental fate (i.e. accumulation, transport, dilution, dispersion). Overall, the present DRASTIC map of South America, in combination with detailed hydrogeological surveys at local scale, may represent a valuable initial step to achieve a sustainable land-use and water management, and in promoting cooperation among states for shared resources, by planning a balanced use of territory and by reducing the anthropic pressure in those areas naturally prone to groundwater leaching.

795

## 796 **Acknowledgments**

797 The authors want to acknowledge Syngenta PS for the financial and material support to this work. We thank  
798 Prof. Ying Fan Reinfelder and Prof. Gonzalo Miguez-Macho for the depth-to-water maps and the fruitful  
799 technical discussions on the quality of data. A special mention is also needed for Prof. Miguel Cooper from  
800 University of São Paulo (ESALQ-USP) and EMBRAPA (Empresa Brasileira de Pesquisa Agropecuária) for

the help in addressing the complexity of soils in Brazil. In addition, we acknowledge the support of CHRIAM Water research center (Project ANID/FONDAP/15130015) for the analysis of Chilean data. Finally, we would like to acknowledge Prof. Everton de Oliveira, Director of Groundwater Project and President of IAH (Brazilian Chapter), for his valuable suggestions, Eng. Roberto Kirchheim for the help in familiarizing ourselves with the extensive hydrogeological datasets of Brazilian Geological Survey (CPRM) and PhD Martina Pacifici for her crucial help in designing and developing the graphical abstract of this paper.

**Supplementary materials.** Additional information related to the article is given in the following supplement file 20211123\_STOTEN\_Supplement\_Rama\_LATAM.docx (link to be added by the journal).

**Data availability.** The high-resolution version of the DRASTIC map of South America, along with the maps of the indexes and the sensitivity analysis, have been archived in a ZENODO repository and can be accessed using the following link: <https://doi.org/10.5281/zenodo.5572252> (Rama et al., 2021). All outcomes have been stored in a .tif format (raster) with different pixel dimensions. Details and specs of graphical outcomes are described in a dedicated file in the same repository (README.txt).

**Author contributions.** The idea of the work was conceived by FR and GB, the data processing was made by FR, GB and LM. The original draft was produced by GB and FR, while the quality data control and internal first review was made by JLA, RH, EEK. Final review, visualization and writing were completed by MM, NC, NK, PS.

**Competing interests.** The authors declare that they have no conflicts of interest.

## References

- Aeschbach-Hertig, W., Gleeson, T., 2012. Regional strategies for the accelerating global problem of groundwater depletion. *Nature Geosci.* 5, 853–861. <https://doi.org/10.1038/ngeo1617>.
- Agudelo Moreno, L. J., Zuleta Lemus, D. D. S., Lasso Rosero, J., Agudelo Morales, D. M., Sepúlveda Castaño, L. M., Paredes Cuervo, D., 2020. Evaluation of aquifer contamination risk in urban expansion areas as a tool for the integrated management of groundwater resources. case: Coffee growing region, Colombia. *Groundw. Sustain. Dev.* 10 <https://doi.org/10.1016/j.gsd.2019.100298>.
- Aller, L., Bennet, T., Lehr, J. H., Petty, R. J., Hachet, G., 1987. DRASTIC: a standardised system for evaluating groundwater pollution potential using hydrogeologic settings (EPA 600/2-87). Environmental Research Laboratory. Office of Research and Development. US Environmental Protection Agency Report. Tucson. 622.
- Alley, W. M., Reilly, T. E., Franke, O. L., 1999. Sustainability of Ground-Water Resources. U.S. Geol. Surv. Circul. 1186. ISBN 0-607-93040-3.
- Aragão, F., Velásquez, L. N. M., Galvão, P., de Castro Tayer, T., Lucon, T. N., de Azevedo, Ú. R., 2020. Natural background levels and validation of the assessment of intrinsic vulnerability to the contamination in the carste lagoa santa protection unit, minas gerais, brazil. *Environ. Earth Sci.* 79(1). <https://doi.org/10.1007/s12665-019-8771-5>.

840 Arumi, J. L., L. Jara., 2009. Cartas de Vulnerabilidad Regiones de O'Higgins y Maule. Essbio S. A.  
841 Concepción. 28. Chile.

842 Ascott, M.J., Gooddy, D.C., Wang, L., Stuart, M.E., Lewis, M.A., Ward, R.S., Binley, A.M., 2017. Global  
843 patterns of nitrate storage in the vadose zone. *Nat. Commun.* 8, 1–6. [https://doi.org/10.1038/s41467-](https://doi.org/10.1038/s41467-017-01321-w)  
844 [017-01321-w](https://doi.org/10.1038/s41467-017-01321-w).

845 Babiker, I. S., Mohamed, M. A. A., Hiyama, T., Kato, K., 2005. A GIS-based DRASTIC model for assessing  
846 aquifer vulnerability in Kakamigahara heights, Gifu prefecture, central Japan. *Sci. Tot. Environ.* 345(1-  
847 3), 127–140. <https://doi.org/10.1016/j.scitotenv.2004.11.005>.

848 Batjes, N. H., Ribeiro, E., van Oostrum, A., 2020. Standardised soil profile data to support global mapping and  
849 modelling (WoSIS snapshot 2019). *Earth Syst. Sci. Data.* 12, 299–320. [https://doi.org/10.5194/essd-12-](https://doi.org/10.5194/essd-12-299-2020)  
850 [299-2020](https://doi.org/10.5194/essd-12-299-2020).

851 Beck, H. E., Zimmermann, N. E., McVicar, T. R., Vergopolan, N., Berg, A., Wood, E. F., 2018. Present and  
852 future köppen-geiger climate classification maps at 1-km resolution. *Sci. Data.* 5.  
853 <https://doi.org/10.1038/sdata.2018.214>.

854 Betancur, T., Palacio, C., Gaviria, J. I., Rueda, M., 2013. Methodological proposal to assess groundwater  
855 contamination danger: study case of Bajo Cauca aquifer (Colombia). *Environ. Earth Sci.* 70, 315–328.  
856 <https://doi.org/10.1007/s12665-012-2129-6>.

857 Bocanegra, E., da Silva Jr., G. C., Custodio, E., Manzano, M., Montenegro, S., 2010. State of knowledge of  
858 coastal aquifer management in South America. *Hydrogeol. J.* 18(1), 261–267.  
859 <https://doi.org/10.1007/s10040-009-0520-5>.

860 Boujon, P., Sanci, R., 2014. Vulnerability assessment of the aquifer in the basin of the el cura stream,  
861 gualeguaychú, entre ríos. *Rev. Asoc. Geol. Argent.* 71(2), 275–291. ISSN 00044822.

862 Busico, G., Cuoco, E., Kazakis, N., Colombani, N., Mastrocicco, M., Tedesco, D., Voudouris, K., 2018.  
863 Multivariate statistical analysis to characterize/discriminate between anthropogenic and geogenic trace  
864 elements occurrence in the Campania Plain, Southern Italy. *Environ. Pollut.* 234, 260–269.  
865 <https://doi.org/10.1016/j.envpol.2017.11.053>.

866 Busico, G., Giuditta, E., Kazakis, N., Colombani, N., 2019. A hybrid GIS and AHP approach for modelling  
867 actual and future forest fire risk under climate change accounting water resources attenuation role.  
868 *Sustainability (Switzerland)*. 11(24). <https://doi.org/10.3390/su11247166>.

869 Busico, G., Kazakis, N., Colombani, N., Mastrocicco, M., Voudouris, K., Tedesco, D., 2017. A modified  
870 SINTACS method for groundwater vulnerability and pollution risk assessment in highly anthropized  
871 regions based on NO<sub>3</sub> – and SO<sub>4</sub><sup>2-</sup> concentrations. *Sci. Total Environ.* 609, 1512–1523.  
872 <https://doi.org/10.1016/j.scitotenv.2017.07.257>.

873 Busico, G., Kazakis, N., Cuoco, E., Colombani, N., Tedesco, D., Voudouris, K., Mastrocicco, M., 2020. A  
874 novel hybrid method of specific vulnerability to anthropogenic pollution using multivariate statistical  
875 and regression analyses. *Water Res.* 171. <https://doi.org/10.1016/j.watres.2019.115386>.

876 Capitanio, F. A., Faccenna, C., Zlotnik, S., Stegman, D. R., 2011. Subduction dynamics and the origin of  
877 Andean orogeny and the Bolivian orocline. *Nature.* 480, 83–86. <https://doi.org/10.1038/nature10596>.

878 Caprario, J., Rech, A. S., Finotti, A. R., 2019. Vulnerability assessment and potential contamination of  
879 unconfined aquifers. *Water Supply.* 19(4), 1008–1016. <https://doi.org/10.2166/ws.2018.147>.

880 Céleri, R., Feyen, J., 2009. The Hydrology of Tropical Andean Ecosystems: Importance, Knowledge Status,  
881 and Perspectives. *Mt. Res. Dev.* 29(4), 350–355. <https://doi.org/10.1659/mrd.00007>.

882 CETESB., 2020. Qualidade das águas subterrâneas no Estado de São Paulo Boletim 2020. São Paulo. 31.  
883 [https://cetesb.sp.gov.br/aguas-subterraneas/wp-content/uploads/sites/13/2021/07/Boletim-de-](https://cetesb.sp.gov.br/aguas-subterraneas/wp-content/uploads/sites/13/2021/07/Boletim-de-Qualidade-da-Aguas-Subterraneas-no-Estado-de-Sao-Paulo-2020.pdf)  
884 [Qualidade-da-Aguas-Subterraneas-no-Estado-de-Sao-Paulo-2020.pdf](https://cetesb.sp.gov.br/aguas-subterraneas/wp-content/uploads/sites/13/2021/07/Boletim-de-Qualidade-da-Aguas-Subterraneas-no-Estado-de-Sao-Paulo-2020.pdf).

885 Civita, M., De Maio, M., 2004. Assessing and mapping groundwater vulnerability to contamination: the Italian  
886 “combined” approach. *Geofis. Int.* 43(4), 513–532. ISSN 0016-7169.

887 Cooper, M., Mendes, L. M. S., Silva, W. L. C., Sparovek, G., 2005. A National Soil Profile Database for Brazil  
888 Available to International Scientists. *Soil Sci. Soc. of Am. J.* 69(3), 649.  
889 <https://doi.org/10.2136/sssaj2004.0140>.

890 CPRM website. <http://geosgb.cprm.gov.br/geosgb/downloads.html> (accessed 12 October 2020).

891 Cuthbert, M. O., Gleeson, T., Moosdorf, N., Befus K. M., Schneider, A., Hartmann, J., Lehner B., 2019. Global  
892 patterns and dynamics of climate–groundwater interactions. *Nat. Clim. Chang.* 9, 137–141.  
893 <https://doi.org/10.1038/s41558-018-0386-4>.

894 Dai, Y., Xin, Q., Wei, N., Zhang, Y., Shangguan, W., Yuan, H., Zhang, S., Liu, S., Lu X., 2019. A global high-  
895 resolution data set of soil hydraulic and thermal properties for land surface modelling. *J. Adv. Model.*  
896 *Earth Syst.* 11, 2996–3023. <https://doi.org/10.1029/2019MS001784>.

897 Davis, G. B., Barber, C., Power, T. R., Thierrin, J., Patterson, B. M., Rayner, J. L., Wu, Q., 1999. The  
898 variability and intrinsic remediation of a BTEX plume in anaerobic sulphate-rich groundwater. *J.*  
899 *Contam. Hydrol.* 36, 265–290. [https://doi.org/10.1016/S0169-7722\(98\)00148-X](https://doi.org/10.1016/S0169-7722(98)00148-X).

900 de Graaf, I. E. M., Sutanudjaja, E. H., van Beek, L. P. H., Bierkens, M. F. P., 2015. A high-resolution global-  
901 scale groundwater model. *Hydrol. Earth Syst. Sci.* 19, 823–837. [https://doi.org/10.5194/hess-19-823-](https://doi.org/10.5194/hess-19-823-2015)  
902 2015.

903 de Graaf, I. E. M., Gleeson, T., (Rens) van Beek, L. P. H., Sutanudjaja, E. H., Bierkens M. F. P., 2019.  
904 Environmental flow limits to global groundwater pumping, *Nature.* 574, 90–94.  
905 <https://doi.org/10.1038/s41586-019-1594-4>.

906 De Sy, V., Herold, M., Achard, F., Beuchle, R., Clevers, J. G. P. W., Lindquist, E., Verchot, L., 2015. Land  
907 use patterns and related carbon losses following deforestation in south America. *Environ. Res. Lett.*  
908 10(12). <https://doi.org/10.1088/1748-9326/10/12/124004>.

909 DGA., 2019. Mapa hidroquímico de Chile. Ministerio de Obras Públicas. Dirección General de Aguas.  
910 División de Conservación de Recursos Hídricos. Santiago, Chile, 111.  
911 <https://snia.mop.gob.cl/sad/CQA5868.pdf>.

912 Dobson, R., Schroth, M. H., Zeyer, J., 2007. Effect of water-table fluctuation on dissolution and biodegradation  
913 of a multi-component, light nonaqueous-phase liquid. *J. Contam. Hydrol.* 94, 235–248.  
914 <https://doi.org/10.1016/j.jconhyd.2007.07.007>.

915 Duhalde, D. J., Arumí, J. L., Oyarzún, R. A., Rivera, D. A., 2018. Fuzzy-based assessment of groundwater  
916 intrinsic vulnerability of a volcanic aquifer in the chilean andean valley. *Environ. Monit. Assess.* 190(7).  
917 <https://doi.org/10.1007/s10661-018-6758-4>.

918 European Union, Copernicus Land Monitoring Service 2018, European Environment Agency (EEA).

919 Fan, Y., Li, H., Miguez-Macho, G., 2013. Global Patterns of Groundwater Table Depth. *Science.* 339(6122),  
920 940–943. <https://doi.org/10.1126/science.1229881>.

921 Fan, Y., Miguez-Macho, G., 2010. Potential groundwater contribution to Amazon evapotranspiration. *Hydrol.*  
922 *Earth Syst. Sci.* 14, 2039–2056. <https://doi.org/10.5194/hess-14-2039-2010>.

923 FAO/IIASA/ISRIC/ISSCAS/JRC., 2012. Harmonized World Soil Database (version 1.2). Rome, Italy and  
924 IIASA, Laxenburg, Austria.

925 Fick, S. E., R. J. Hijmans., 2017. WorldClim 2: new 1km spatial resolution climate surfaces for global land  
926 areas. *Int. J. Climatol.* 37(12), 4302–4315. <https://doi.org/10.1002/joc.5086>.

927 Foster, S., 1987. Fundamental concepts in aquifer vulnerability, pollution risk and protection strategy.  
928 International Conference, Noordwijk Aan Zee. TNO Proc. Inf. 38, 69–86.

929 Foster, S., Hirata, R., 1988. Groundwater pollution risk assessment: a methodology using available data.  
930 WHO-PAHO-CEPIS. Lima.

931 Foster, S., Hirata, R., Andreo, B., 2013. Le concept de vulnérabilité des aquifères à la pollution: Une aide ou  
932 un obstacle au renforcement de leur protection? *Hydrogeol. J.* 21, 1389–1392.  
933 <https://doi.org/10.1007/s10040-013-1019-7>.

934 Fritch, T. G., McKnight, C. L., Yelderman Jr., J. C., Arnold, J. G., 2000. An aquifer vulnerability assessment  
935 of the paluxy aquifer, central texas, USA, using GIS and a modified DRASTIC approach. *Environ.*  
936 *Manage.* 25(3), 337–345. <https://doi.org/10.1007/s002679910026>.

937 Garreaud, R. D., 2009. The Andes climate and weather. *Adv. Geosci.* 22, 3–11. [https://doi.org/10.5194/adgeo-](https://doi.org/10.5194/adgeo-22-3-2009)  
938 22-3-2009.

939 Garreaud, R. D., Vuille, M., Compagnucci, R., Marengo, J., 2009. Present-day South American climate.  
940 *Palaeogeogr. Palaeoclimatol. Palaeoecol.* 281(3-4), 180–195.  
941 <https://doi.org/10.1016/j.palaeo.2007.10.032>.

942 Giacomazzo, A. P., de Almeida, W. S., 2020. Study of the contamination potential of the jockey club landfill,  
943 distrito federal, brazil. *Eng. Sanit. e Ambient.* 25(6), 909–920. [https://doi.org/10.1590/s1413-](https://doi.org/10.1590/s1413-4152202020180223)  
944 4152202020180223.

945 Gimsing, A.L., Agert, J., Baran, N., Boivin A., Ferrari, F., Gibson, R., Hammond, L., Hegler, F., Jones, R. L.,  
946 Konig, W., Kreuger, J., van der Linden, T., Liss, D., Loiseau, L., Massey, A., Miles, B., Monrozies L.,  
947 Newcombe, A., Poot, A., Reeves, G. L., Reichenberger, S., Rosenbom, A. E., Staudenmaier, H., Sur,  
948 R., Shwen, A., Stemmer, M., Tuting, W., Ulrich, U., 2019. Conducting groundwater monitoring studies  
949 in Europe for pesticide active substances and their metabolites in the context of Regulation (EC)  
950 1107/2009. *J. Consum. Prot. Food. Saf.* 14, 1–93. <https://doi.org/10.1007/s00003-019-01211-x>.

951 Giri C. and Long, J., 2014. Land Cover Characterization and Mapping of South America for the Year 2010  
952 Using Landsat 30 m Satellite Data. *Remote Sens.* 6(10), 9494–9510. <https://doi.org/10.3390/rs6109494>.

953 Gleeson, T. N., Moosdorf, J., Hartmann, L. P. H. van Beek., 2014. A glimpse beneath earth’s surface: Global  
954 HYdrogeology MaPS (GLHYMPS) of permeability and porosity. *Geophys. Res. Lett.* 41, 3891–3898.  
955 <https://doi.org/10.1002/2014GL059856>.

956 Gleeson, T., VanderSteen, J., Sophocleous, M. A., Tanigauchi, M., Alley W. M., Allen, D. M., Zhou, Y., 2010.  
957 Groundwater sustainability strategies. *Nature Geosci.* 3, 378–379. <https://doi.org/10.1038/ngeo881>.

958 Gogu, R. C., Dassargues, A., 2000. Current trends and future challenges in groundwater vulnerability  
959 assessment using overlay and index methods. *Environ. Geol.* 39(6), 549–559. [https://doi-](https://doi-org/10.1007/s002540050466)  
960 [org/10.1007/s002540050466](https://doi.org/10.1007/s002540050466).

961 Gomes, M. C. R., Mendonça, L. A. R., Cavalcante, I. N., 2018. Mapping of vulnerability and risk of  
962 groundwater pollution in the eastern portion of the araripe sedimentary basin, ceará, Brasil. *Anu. do*  
963 *Inst. De Geocienc.* 41(3), 252–259. [https://doi.org/10.11137/2018\\_3\\_252\\_259](https://doi.org/10.11137/2018_3_252_259).

964 Gómez, J., Schobbenhaus, C., Montes, N. E., compilers., 2019. Geological Map of South America 2019, Scale  
965 1:5 000 000, Commission for the Geological Map of the World (CGMW). Colombian Geol. Surv. and  
966 Geol. Surv. of Brazil. Paris. <https://doi.org/10.32685/10.143.2019.929>.

967 Goode, D. J., Konikow, L. F., 1990. Apparent dispersion in transient groundwater flow. *Water Resour. Res.*  
968 26, 2339–2351. <https://doi.org/10.1029/WR026i010p02339>.

969 Goyal, D., Haritash, A. K., Singh, S. K. (2021). A comprehensive review of groundwater vulnerability  
970 assessment using index-based, modelling, and coupling methods. *J. Environ. Manag.* 296  
971 <https://doi.org/10.1016/j.jenvman.2021.113161>.

972 Hendrickx, J. M., Flury, M., 2001. Uniform and preferential flow mechanisms in the vadose zone, in:  
973 Conceptual models of flow and transport in the fractured vadose zone. National Research Council. 149–  
974 187. Washington, DC: The National Academies Press. <https://doi.org/10.17226/10102>.

975 Herlinger, R., Viero, A. P., 2007. Groundwater vulnerability assessment in coastal plain of Rio Grande do Sul  
976 State, Brazil, using drastic and adsorption capacity of soils. *Environ. Geol.* 52, 819–829.  
977 <https://doi.org/10.1007/s00254-006-0518-4>.

978 Hirata, R. C. A., Bastos, C. R. A., Rocha, G. A., Gomes, D. C., Iritani, M. A., 1991. Groundwater pollution  
979 risk and vulnerability map of the state of sao paulo, Brazil. *Water Sci. Technol.* 24(11), 159–169.  
980 <https://doi.org/10.2166/wst.1991.0348>.

981 Hu, X., Ma, C., Qi, H., Guo, X., 2018. Groundwater vulnerability assessment using the GALDIT model and  
 982 the improved DRASTIC model: a case in Weibei Plain, China. *Environ. Sci. Pollut. Res.* 25(32), 32524–  
 983 32539. <https://doi.org/10.1007/s11356-018-3196-3>.

984 Huan, H., Jinsheng, W., Yanguo, T., 2012. Assessment and validation of groundwater vulnerability to nitrate  
 985 based on a modified DRASTIC model: a case study in Jilin City of northeast China. *Sci. Total Environ.*  
 986 440, 14–23. <https://doi.org/10.1016/j.scitotenv.2012.08.037>.

987 Huscroft, J., Gleeson, T., Hartmann, J., Börker, J., 2018. Compiling and mapping global permeability of the  
 988 unconsolidated and consolidated Earth: GLobal HYdrogeology MaPS 2.0 (GLHYMPS 2.0). *Geophys.*  
 989 *Res. Lett.* 45, 1897–1904. <https://doi.org/10.1002/2017GL075860>.

990 IGRAC (International Groundwater Resources Assessment Centre) and UNESCO-IHP (UNESCO  
 991 International Hydrological Programme), 2015. *Transboundary Aquifers of Latin America, Based on:*  
 992 *Transboundary Aquifers of the World, Map*, Delft, Netherlands.

993 Jahromi, M. N., Gomeh, Z., Busico, G., Barzegar, R., Samany, N. N., Aalami, M. T., Tedesco, D., Mastrocicco,  
 994 M., Kazakis, N., 2021. Developing a SINTACS-based method to map groundwater multi-pollutant  
 995 vulnerability using evolutionary algorithms. *Environ. Sci. Pollut. Res.* 28(7), 7854–7869.  
 996 <https://doi.org/10.1007/s11356-020-11089-0>.

997 Jarvis, N. J., 2007. A review of non-equilibrium water flow and solute transport in soil macropores: principles,  
 998 controlling factors and consequences for water quality. *Eur. J. Soil Sci.* 58. 3.  
 999 <https://doi.org/10.1111/j.1365-2389.2007.00915.x>.

1000 Jasechko, S., Perrone, D., Befus, K., Cardenas, M. B., Ferguson, G., Gleeson, T., Luijendijk, E., McDonnell,  
 1001 J. J., Taylor, R. G., Wada, Y., Kirchner, J. W., 2017. Global aquifers dominated by fossil groundwaters  
 1002 but wells vulnerable to modern contamination. *Nature Geosci.* 10, 425–429.  
 1003 <https://doi.org/10.1038/ngeo2943>.

1004 Jasechko, S., S. J. Birks, T. Gleeson, Y. Wada, P. J. Fawcett, Z. D. Sharp, J. J. McDonnell, J. M. Welker.,  
 1005 2014. The pronounced seasonality of global groundwater recharge. *Water Resour. Res.* 50, 8845–8867.  
 1006 <https://doi.org/10.1002/2014WR015809>.

1007 Javadi, S., Hashemy Shahdany, S. M., Neshat, A., Chambel, A. (2020). Multi-parameter risk mapping of  
 1008 qazvin aquifer by classic and fuzzy clustering techniques. *Geocarto Int.*  
 1009 <https://doi.org/10.1080/10106049.2020.1778099>.

1010 Jia, Z., Bian, J., Wang, Y., Wan, H., Sun, X., Li, Q., 2019. Assessment and validation of groundwater  
 1011 vulnerability to nitrate in porous aquifers based on a DRASTIC method modified by projection pursuit  
 1012 dynamic clustering model. *J. C. Hydrol.* 226. <https://doi.org/10.1016/j.jconhyd.2019.103522>.

1013 Kazakis, N., Busico, G., Colombani, N., Mastrocicco, M., Pavlou, A., Voudouris, K., 2019. GALDIT-SUSI a  
 1014 modified method to account for surface water bodies in the assessment of aquifer vulnerability to  
 1015 seawater intrusion. *J. Environ. Manage.* 235, 257–265. <https://doi.org/10.1016/j.jenvman.2019.01.069>.

1016 Kazakis, N., Voudouris, K. S., 2015. Groundwater vulnerability and pollution risk assessment of porous  
 1017 aquifers to nitrate: Modifying the DRASTIC method using quantitative parameters. *J. Hydrol.* 525, 13–  
 1018 25. <https://doi.org/10.1016/j.jhydrol.2015.03.035>.

1019 Keuskamp, J. A., Van Drecht, G., Bouwman, A. F., 2012. European-scale modelling of groundwater  
 1020 denitrification and associated N<sub>2</sub>O production. *Environ. Pollut.* 165, 67–76.  
 1021 <https://doi.org/10.1016/j.envpol.2012.02.008>.

1022 Konikow, L. F., Kendy, E., 2005. Groundwater depletion: A global problem. *Hydrogeol. J.* 13, 317–320.  
 1023 <https://doi.org/10.1007/s10040-004-0411-8>.

1024 Kumar, R., Heße, F., Rao, P. S. C., Musolff, A., Jawitz, J. W., Sarrazin, F., Samaniego, L., Fleckenstein, J. H.,  
 1025 Rakovec, O., Thober, S., Attinger, S., 2020. Strong hydroclimatic controls on vulnerability to subsurface  
 1026 nitrate contamination across Europe. *Nat. Commun.* 11(1). [https://doi.org/10.1038/s41467-020-19955-](https://doi.org/10.1038/s41467-020-19955-8)  
 1027 8.

1028 Lasagna, M., De Luca, D. A., Franchino, E., 2016. The role of physical and biological processes in aquifers  
1029 and their importance on groundwater vulnerability to nitrate pollution. *Environ. Earth Sci.* 75, 961.  
1030 <https://doi.org/10.1007/s12665-016-5768-1>.

1031 Li, R., Merchant, J. W., 2013. Modeling vulnerability of groundwater to pollution under future scenarios of  
1032 climate change and biofuels-related land use change: A case study in north dakota, USA. *Sci. Total*  
1033 *Environ.* 447, 32–45. <https://doi.org/10.1016/j.scitotenv.2013.01.011>.

1034 Lima, M. L., Zelaya, K., Massone, H., 2011. Groundwater vulnerability assessment combining the drastic and  
1035 dyna-CLUE model in the argentine pampas. *Environ. Manage.* 47(5), 828–839.  
1036 <https://doi.org/10.1007/s00267-011-9652-1>.

1037 Lodwick, W. A., Monson, W., Svoboda, L., 1990. Attribute error and sensitivity analysis of map operations in  
1038 geographical in-formation systems: Suitability analysis. *Int. J. Geogr. Inf. Syst.* 4(4), 413–428.  
1039 <https://doi.org/10.1080/02693799008941556>.

1040 Machiwal, D., Cloutier, V., Güler, C. Kazakis, N., 2018. A review of GIS-integrated statistical techniques for  
1041 groundwater quality evaluation and protection. *Environ. Earth Sci.* 77, 681.  
1042 <https://doi.org/10.1007/s12665-018-7872-x>.

1043 Machiwal, D., Jha, M. K., Singh, V. P., Mohan, C., 2018. Assessment and mapping of groundwater  
1044 vulnerability to pollution: Current status and challenges. *Earth-Sci. Rev.* 185, 901–927.  
1045 <https://doi.org/10.1016/j.earscirev.2018.08.009>.

1046 Massone, H. E. Barilari, A., 2020. Groundwater pollution: A discussion about vulnerability, hazard and risk  
1047 assessment. *Hydrogeol. J.* 28(2), 463–466. <https://doi.org/10.1007/s10040-019-02090-0>.

1048 Massone, H., Londoño, M. Q., Martínez, D., 2010. Enhanced groundwater vulnerability assessment in  
1049 geological homogeneous areas: A case study from the argentine pampas. *Hydrogeol. J.* 18(2), 371–379.  
1050 <https://doi.org/10.1007/s10040-009-0506-3>.

1051 Miguez-Macho, G. Fan, Y., 2012. The role of groundwater in the Amazon water cycle: 1. Influence on seasonal  
1052 streamflow, flooding and wetlands. *J. Geophys. Res.* 117, D15113.  
1053 <https://doi.org/10.1029/2012JD017539>.

1054 Miguez-Macho, G. Fan, Y., 2012. The role of groundwater in the Amazon water cycle: 2. Influence on seasonal  
1055 soil moisture and evapotranspiration. *J. Geophys. Res.* 117, D15114.  
1056 <https://doi.org/10.1029/2012JD017540>.

1057 Mohan, C., Western, A. W., Wei, Y., Saft, M., 2018. Predicting groundwater recharge for varying land cover  
1058 and climate conditions – a global meta-study. *Hydrol. Earth Syst. Sci.* 22, 2689–2703.  
1059 <https://doi.org/10.5194/hess-22-2689-2018>.

1060 Montoya, J. C., Porfiri, C., Roberto, Z. E., Viglizzo, E. F., 2019. Assessing the vulnerability of groundwater  
1061 resources in semiarid lands of central argentina. *Sustain. Water Resour. Manag.* 5(4), 1419–1434.  
1062 <https://doi.org/10.1007/s40899-018-0246-4>.

1063 Muñoz Sabater, J., 2019. ERA5-Land hourly data from 1981 to present. Copernicus Climate Change Service  
1064 (C3S) Climate Data Store (CDS). <https://doi.org/10.24381/cds.e2161bac>.

1065 Nadiri, A. A., Sedghi, Z., Khatibi, R., Sadeghfam, S. (2018). Mapping specific vulnerability of multiple  
1066 confined and unconfined aquifers by using artificial intelligence to learn from multiple DRASTIC  
1067 frameworks. *J. Environ. Manag.* 227, 415–428. <https://doi.org/10.1016/j.jenvman.2018.08.019>.

1068 Napolitano, P., Fabbri, A., 1996. Single-Parameter Sensitivity Analysis for Aquifer Vulnerability Assessment  
1069 Using DRASTIC and SINTACS, in: *Proceedings of Vienna Conference, HydroGIS 96: Application of*  
1070 *Geographical Information Systems in Hydrology and Water Resources Management.* IAHS Pub.,  
1071 Vienna, 235, 559–566.

1072 National Research Council (NRC)., 1993. Ground Water Vulnerability Assessment: Predicting Relative  
1073 Contamination Potential Under Conditions of Uncertainty. The National Academies Press, 224.  
1074 Washington, DC: The National Academies Press, <https://doi.org/10.17226/2050>.

- 1075 Neshat, A., Pradhan, B., Pirasteh, S., & Shafri, H. Z. M., 2014. Estimating groundwater vulnerability to  
1076 pollution using a modified DRASTIC model in the Kerman agricultural area, Iran. *Environ. Earth Sci.*  
1077 71(7), 3119–3131. <https://doi.org/10.1007/s12665-013-2690-7>.
- 1078 Nistor, M., 2020. Groundwater vulnerability in Europe under climate change. *Quat. Int.* 547, 185–196.  
1079 <https://doi.org/10.1016/j.quaint.2019.04.012>.
- 1080 Nobre, R. C. M., Rotunno Filho, O. C., Mansur, W. J., Nobre, M. M. M., Cosenza, C. A. N., 2007. Groundwater  
1081 vulnerability and risk mapping using GIS, modeling and a fuzzy logic tool. *J. Contam. Hydrol.* 94(3-4),  
1082 277–292. <https://doi.org/10.1016/j.jconhyd.2007.07.008>.
- 1083 Núñez, C., Verbist, K., 2018. *Atlas de Sequía de América Latina y el Caribe*, UNESCO and CAZALAC. 204.  
1084 ISBN: 978-92-3-300097-1.
- 1085 Oki, T., Kanae, S., 2006. Global hydrological cycles and world water resources. *Science.* 313, 1068–1072.  
1086 <https://www.jstor.org/stable/3847070>.
- 1087 Ottoni, M. V., Ottoni Filho, T. B., Schaap, M. G., Lopes-Assad, M. L. R. C., Rotunno Filho, O. C., 2018.  
1088 Hydrophysical Database for Brazilian Soils (HYBRAS) and Pedotransfer Functions for Water  
1089 Retention. *Vadose Zone J.* 17(1), 0. <https://doi.org/10.2136/vzj2017.05.0095>.
- 1090 Ouedraogo, I., Defourny, P., Vanclooster, M., 2016. Mapping the groundwater vulnerability for pollution at  
1091 the pan african scale. *Sci. Total Environ.* 544, 939–953. <https://doi.org/10.1016/j.scitotenv.2015.11.135>.
- 1092 Pacheco, F. A. L., Pires, L. M. G. R., Santos, R. M. B., Sanches Fernandes, L. F., 2015. Factor weighting in  
1093 DRASTIC modeling. *Sci. Tot. Environ.* 505, 474–486. <https://doi.org/10.1016/j.scitotenv.2014.09.092>.
- 1094 Peixoto da Silva, F., Cavalcante, I. N., 2019. Aquifer vulnerability and contamination risk of groundwater in  
1095 urban environment. *Geologia USP - Serie Científica.* 19(2), 29–40. <https://doi.org/10.11606/issn.2316-9095.v19-142384>.  
1096
- 1097 Rahmani, B., Javadi, S., Shahdany, S. M. H. (2021). Evaluation of aquifer vulnerability using PCA technique  
1098 and various clustering methods. *Geocarto Int.* 36(18), 2117–2140.  
1099 <https://doi.org/10.1080/10106049.2019.1690057>.
- 1100 Rama F., Busico G., Arumi J. L., Kazakis N., Colombani N., Marfella L., Hirata R., Kruse E. E., Sweeney P.,  
1101 and Mastrocicco, M., 2021. DATASETS and OUTCOMES - Assessment of intrinsic aquifer  
1102 vulnerability at continental scale through a critical application of the DRASTIC method: the case of  
1103 South America (version 1.0) [Data set]. Zenodo.
- 1104 Rama, F., Ramos, D. T., Müller, J. B., Corseuil, H. X., Miotliński K., 2019. Flow field dynamics and high  
1105 ethanol content in gasohol blends enhance BTEX migration and biodegradation in groundwater. *J.*  
1106 *Contam. Hydrol.* <https://doi.org/10.1016/j.jconhyd.2019.01.003>.
- 1107 Richts A., Struckmeier W. F., Zaepke M., 2011. WHYMAP and the Groundwater Resources Map of the World  
1108 1:25,000,000. In: Jones J. (eds) *Sustaining Groundwater Resources*. International Year of Planet Earth.  
1109 Springer, Dordrecht. [https://doi.org/10.1007/978-90-481-3426-7\\_10](https://doi.org/10.1007/978-90-481-3426-7_10)
- 1110 Roy-Roura, M., Nolan, B.T., Menció, A., Mas-Pla, J., 2013. Regression model for aquifer vulnerability  
1111 assessment of nitrate pollution in the Osona region (NE Spain). *J. Hydrol.* 505, 150–162.  
1112 <https://doi.org/10.1016/j.jhydrol.2013.09.048>.
- 1113 Sadeghfam, S., Khatibi, R., Nadiri, A. A., Ghodsi, K (2021). Next Stages in Aquifer Vulnerability Studies by  
1114 Integrating Risk Indexing with Understanding Uncertainties by using Generalised Likelihood  
1115 Uncertainty Estimation. *Expo. Health.* 13, 375–389. <https://doi.org/10.1007/s12403-021-00389-6>.
- 1116 Seabra, V. S., Da Silva Jr., G. C., Cruz, C. B. M., 2009. The use of geoprocessing to assess vulnerability on  
1117 the east coast aquifers of rio de janeiro state. *Brazil. Environ. Geol.* 57(3), 665–674.  
1118 <https://doi.org/10.1007/s00254-008-1345-6>.
- 1119 Shangguan, W., T. Hengl, J. Mendes de Jesus, H. Yuan, Y. Dai., 2017. Mapping the global depth to bedrock  
1120 for land surface modeling. *J. Adv. Model. Earth Syst.* 9, 65–88. <https://doi.org/10.1002/2016MS000686>.

1121 Siebert, S., Burke, J., Faures, J. M., Frenken, K., Hoogeveen, J., Döll, P., Portmann, F. T., 2010. Groundwater  
1122 use for irrigation – a global inventory. *Hydrol. Earth Syst. Sci.* 14, 1863–1880.  
1123 <https://doi.org/10.5194/hess-14-1863-2010>.

1124 Stigter, T. Y., Ribeiro, L., Carvalho Dill, A. M. M., 2006. Evaluation of an intrinsic and a specific vulnerability  
1125 assessment method in comparison with groundwater salinization and nitrate contamination levels in two  
1126 agricultural regions in the South of Portugal. *Hydrogeol. J.* 14, 79–99. [https://doi.org/10.1007/S10040-](https://doi.org/10.1007/S10040-004-0396-3)  
1127 [004-0396-3](https://doi.org/10.1007/S10040-004-0396-3).

1128 Sutanudjaja, E. H., van Beek, R., Wanders, N., Wada, Y., Bosmans, J. H. C., Drost, N., van der Ent, R. J., de  
1129 Graaf, I. E. M., Hoch, J. M., de Jong, K., Karssenbergh, D., López López, P., Peßenteiner, S., Schmitz,  
1130 O., Straatsma, M. W., Vannamettee, E., Wissler, D., Bierkens, M. F. P., 2018. PCR-GLOBWB 2: a  
1131 5 arcmin global hydrological and water resources model. *Geosci. Model Dev.* 11, 2429–2453.  
1132 <https://doi.org/10.5194/gmd-11-2429-2018>.

1133 Tayer, T. D., Velásques, L. N. M., 2017. Assessment of intrinsic vulnerability to the contamination of karst  
1134 aquifer using the COP method in the Carste Lagoa Santa Environmental Protection Unit, Brazil.  
1135 *Environ. Earth Sci.* 76, 445, <https://doi.org/10.1007/s12665-017-6760-0>.

1136 Tobler, W., 1987. “Measuring Spatial Resolution”, in: *Proceedings, Land Resources Information Systems*  
1137 *Conference*. Beijing, China. 12–16.

1138 van der Heijden, G., Legout, A., Pollier, B., Bréchet, C., Ranger, J., Dambrine, E., 2013. Tracing and modeling  
1139 preferential flow in a forest soil—Potential impact on nutrient leaching. *Geoderma*. 195, 12–22.  
1140 <https://doi.org/10.1016/j.geoderma.2012.11.004>.

1141 Van Stemproot, D., Ewert, L., Wassenaar, L., 1993. Aquifer vulnerability index: a GIS compatible method for  
1142 groundwater vulnerability mapping. *Can. Water Resour. J.* 18(1), 25–37.  
1143 <https://doi.org/10.4296/cwrj1801025>.

1144 Vanderborght J., Timmerman A., Feyen J., 2020. Solute Transport for Steady-State and Transient Flow in  
1145 Soils with and without Macropores. *Soil Sci. Soc. Am. J.* 64, 4.  
1146 <https://doi.org/10.2136/sssaj2000.6441305x>.

1147 Vías J., Andreo B., Perles M., Carrasco F., Vadillo I., Jiménez P., 2006. Proposed method for groundwater  
1148 vulnerability mapping in carbonate (karstic) aquifers: the COP method. *Hydrogeol. J.* 14, 912–925.  
1149 <https://doi.org/10.1007/s10040-006-0023-6>.

1150 Villar, P.C., 2016. International cooperation on transboundary aquifers in South America and the Guarani  
1151 Aquifer case. *Rev. Bras. de Política Int.* 59. <https://doi.org/10.1590/0034-7329201600107>.

1152 Vu, T. D., Ni, C. F., Li, W. C., Truong M. H. J. W., 2019. Modified index-overlay method to assess spatial–  
1153 temporal variations of groundwater vulnerability and groundwater contamination risk in areas with  
1154 variable activities of agriculture developments. *Water*. 11 (12). <https://doi.org/10.3390/w11122492>.

1155 Wachniew, P., Zurek, A. J., Stumpp, C., Gemitzi, A., Gargini, A., Filippini, M., Rozanski, K., Meeks, J.,  
1156 Kværner, J. Witczak, S., 2016. Toward operational methods for the assessment of intrinsic groundwater  
1157 vulnerability: A review. *Crit. Rev. Environ. Sci. Technol.* 46(9), 827–884.  
1158 <https://doi.org/10.1080/10643389.2016.1160816>.

1159 Yamazaki, D., Ikeshima, D., Tawatari, R., Yamaguchi, T., O’Loughlin, F., Neal, J. C., Sampson, C.C., Kanae,  
1160 S., Bates, P. D., 2017. A high-accuracy map of global terrain elevations. *Geophys. Res. Lett.* 44(11),  
1161 5844–5853. <https://doi.org/10.1002/2017gl072874>.

1162 Yin, L., Zhang, E., Wang, X., Wenninger, J., Dong, J., Guo, L., Huang, J., 2013. A GIS-based DRASTIC  
1163 model for assessing groundwater vulnerability in the ordos plateau, China. *Environ. Earth Sci.* 69(1),  
1164 171–185. <https://doi.org/10.1007/s12665-012-1945-z>.

1165 Yoon, JH. Zeng, N., 2010. An Atlantic influence on Amazon rainfall. *Clim. Dyn.* 34, 249–264.  
1166 <https://doi.org/10.1007/s00382-009-0551-6>.